A&A 516, A55 (2010)
DOI: 10.1051/0004-6361/200913451

Astronomy & Astrophysics

Properties of stellar generations in globular clusters and relations with global parameters⋆,⋆⋆

E. Carretta[1], A. Bragaglia[1], R. G. Gratton[2], A. Recio-Blanco[3], S. Lucatello[2,4], V. D'Orazi[2], and S. Cassisi[5]

[1] INAF – Osservatorio Astronomico di Bologna, via Ranzani 1, 40127 Bologna, Italy
e-mail: eugenio.carretta@oabo.inaf.it
[2] INAF – Osservatorio Astronomico di Padova, vicolo dell'Osservatorio 5, 35122 Padova, Italy
[3] Laboratoire Cassiopée UMR 6202, Université de Nice Sophia-Antipolis, CNRS, Observatoire de la Côte d'Azur, BP 4229, 06304 Nice Cedex 4, France
[4] Excellence Cluster Universe, Technische Universität München, Boltzmannstr. 2, 85748 Garching, Germany
[5] INAF – Osservatorio Astronomico di Collurania, via M. Maggini, 64100 Teramo, Italy

Received 12 October 2009 / Accepted 2 March 2010

ABSTRACT

We revise the scenario of the formation of Galactic globular clusters (GCs) by adding the observed detailed chemical composition of their different stellar generations to the set of their global parameters. We exploit the unprecedented set of homogeneous abundances of more than 1200 red giants in 19 clusters, as well as additional data from literature, to give a new definition of *bona fide* GCs, as the stellar aggregates showing the Na-O anticorrelation. We propose a classification of GCs according to their kinematics and location in the Galaxy in three populations: disk/bulge, inner halo, and outer halo. We find that the luminosity function of GCs is fairly independent of their population, suggesting that it is imprinted by the formation mechanism only marginally affected by the ensuing evolution. We show that a large fraction of the primordial population should have been lost by the proto-GCs. The extremely low Al abundances found for the primordial population of massive GCs indicate a very fast enrichment process before the formation of the primordial population. We suggest a scenario for the formation of GCs that includes at least three main phases: i) the formation of a precursor population (likely due to the interaction of cosmological structures similar to those that led to the formation of dwarf spheroidals, but residing at smaller Galactocentric distances, with the early Galaxy or with other structures); ii) the triggering of a long episode of star formation (the primordial population) from the precursor population; and iii) the formation of the current GC, mainly within a cooling flow formed by the slow winds of a fraction of the primordial population. The precursor population is very effective in raising the metal content in massive and/or metal-poor (mainly halo) clusters, while its rôle is minor in small and/or metal-rich (mainly disk) ones. Finally, we use principal component analysis and multivariate relations to study the phase of metal enrichment from first to second generation. We conclude that most of the chemical signatures of GCs may be ascribed to a few parameters, the most important being metallicity, mass, and cluster age. Location within the Galaxy (as described by the kinematics) also plays some rôle, while additional parameters are required to describe their dynamical status.

Key words. stars: abundances – stars: atmospheres – stars: Population II – globular clusters: general

1. Introduction

The assembly of the early stellar populations in galaxies is one of the hottest open issues in astronomy. Globular clusters (GCs) are a major component of these old stellar populations. They are easily detectable and can be studied in some detail even at large distances, providing a potentially powerful link between external galaxies and local stellar populations. A clear comprehension of those mechanisms that led to the formation and evolution of GCs and of the relations existing between GCs and field stars is a basic requirement for understanding how galaxies assemble (see e.g. Bekki et al. 2008). Various authors have proposed scenarios for the formation of GCs (Peebles & Dicke 1968; Searle & Zinn 1978; Fall & Rees 1985; Cayrel 1986; Freeman 1990; Brown et al. 1991, 1995; Ashman & Zepf 1992; Murray & Lin 1992; Bromm & Clarke 2002; Kravtsov & Gnedin 2005; Saitoh et al. 2006; Bekki & Chiba 2002, 2007; Bekki et al. 2007; Hasegawa et al. 2009; Marcolini et al. 2009; Hartwick 2009). While very suggestive and intriguing, these scenarios either do not convincingly reproduce the whole spectrum of observations, or are likely to be incomplete, describing only part of the sequence of events that lead to GC formation or only a subset of them. We still lack the clear understanding we would need; however, some recent progress is opening new promising perspectives.

For almost forty years, we have known that large star-to-star abundance variations for several light elements are present in GCs (see Gratton et al. 2004, for a recent review). Regarded for a long time as intriguing abundance "anomalies" restricted to some cluster stars, the observed peculiar chemical composition only recently was explicitly understood as a universal phenomenon in GCs, most likely related to their very same nature/origin (Carretta 2006; Carretta et al. 2006, Paper I). The observational pattern of Li, C, N, O, Na, Al, Mg in cluster stars has currently been assessed (see e.g. the review by Gratton et al. 2004), thanks to several important milestones:

(i) Variations for the heavier species (O, Na, Mg, Al) are restricted to the denser cluster environment. The signature for other elements (Li, C, N) may be reproduced by

⋆ Based on observations collected at ESO telescopes under programmes 072.-D0507 and 073.D-0211.
⋆⋆ Appendix A is only available in electronic form at http://www.aanda.org

assuming a mixture of primordial composition plus evolutionary changes. The latter were caused by two mixing episodes, occurring at the end of the main sequence (the first dredge-up) and after the bump on the red giant branch (RGB), both in low-mass Population II field stars and in their cluster analogues (Charbonnel et al. 1998; Gratton et al. 2000b; Smith & Martell 2003).

(ii) The observed pattern of abundance variations is established in proton-capture reactions of the CNO, NeNa, and MgAl chains during H-burning at high temperature (Denisenkov & Denisenkova 1989; Langer et al. 1993).

(iii) The variations are also found among unevolved stars currently on the main sequence (MS) of GCs (Gratton et al. 2001; Ramirez & Cohen 2002; Carretta et al. 2004; D'Orazi et al. 2010). This unequivocally implies that this composition *has been imprinted in the gas by a previous generation of stars*. The necessity of this conclusion stems from low-mass MS stars not being able to reach the high temperatures for the nucleosynthetic chains required to produce the observed inter-relations between the elements (in particular the Mg-Al anticorrelation). This calls for a class of now extinct stars, more massive than the low-mass ones presently evolving in GCs, as the site for the nucleosynthesis.

Unfortunately, we do not yet know what kind of stars produced the pollution. The most popular candidates are either intermediate-mass AGB stars (e.g., D'Antona & Ventura 2007) or very massive, rotating stars (FRMS, e.g., Decressin et al. 2007)[1].

The observed abundance variations are also connected to the He abundance, since He is the main outcome of H-burning (i.e., Na-rich, O-poor stars should also be He-rich). However, the relation between He abundance variations and the light element abundance pattern may be quite complicated. Multiple main sequences attributed to populations with different He fraction Y have recently been found in some GCs (ω Cen, see Bedin et al. 2004, and NGC 2808, Piotto et al. 2007). We have found a clear indication that Na-rich and Na-poor stars in NGC 6218 and NGC 6752 have slightly different RGB-bump luminosities (Carretta et al. 2007b, hereinafter Paper III), as expected from models of cluster subpopulations with different He content (Salaris et al. 2006). In separate papers (Gratton et al. 2010; Bragaglia et al. 2010), we examined the relation between He and light element abundance variations from evidence based on horizontal branch (HB) and RGB.

In summary, GCs are not exactly a simple stellar population, because they must harbour at least *two stellar generations*, as explained above, that are clearly distinct by their chemistry. These populations may be separated, provided data of adequate quality are available. The patterns of anticorrelated Na-O and Mg-Al and, partly, C-N and Li-Na (and associated correlations) must be regarded as the fingerprints of these different subpopulations, and may be used to get insight into the early phases of formation and evolution of GCs, which are still obscure. The timescale for the release of matter processed by H-burning at high temperature is of the order of 10^7 yr if it comes from FMRS and a few times longer if it comes from massive AGB stars. Thus, whatever the candidate producers, the observed patterns were certainly already in place within some 10^8 yr after the start of cluster formation. These processes occurred on timescales less than 1% of the typical total age of a GC. The dynamical evolution that occurred in the remaining 99% of the cluster lifetime, while likely important, did not completely erase these fingerprints. Their fossil record is still recognisable in the chemical composition of the low-mass stars.

To decipher the relevant information we need large and homogeneous data sets, like the one we have recently gathered (Carretta et al. 2009a,b). The goal of the present paper is to exploit this wealth of data to discuss the abundance patterns of the different populations within each GC. We correlate them with global cluster parameters, such as the HB morphology and structural or orbital parameters. This will allow a better understanding of the main properties of the stellar populations of GCs, hence getting insight into the early phases of their evolution. Using this information as a guide, we sketch a quite simple scenario for the formation of GCs, which is essentially an updated and expanded version of what was proposed more than thirty years ago by Searle & Zinn (1978). This scenario naturally explains the relation between GCs and other small systems (dwarf Spheroidals: dSphs), and suggests a connection between GCs and field stars. In fact, we propose that the primordial population of GCs might be the main building block of the halo, although other components are likely present.

The present paper is organised as follows. In Sect. 2 we give a brief summary of our previous work to set the stage for the following discussion. In Sect. 3 we recall some general properties of the GC population and the division into subpopulations; we also present the selection criteria for our sample, discussing possible biases, and the parameters used in the analysis. In Sect. 4 we discuss the properties of the first stellar generation, and we present a scenario for GC formation. In Sect. 5 we consider the second phase of chemical enrichment in GCs, comparing the properties of the second generation with those of the primordial one and presenting a number of interesting correlations. Finally, in Sect. 6, we more generally discuss the correlations with global GC parameters and give a summary and our conclusions. In the Appendix, we present a new classification of all Galactic GCs, dividing them into disk/bulge, inner halo, and outer halo ones on a kinematical basis and list their metallicities on the scale defined in Carretta et al. (2009c), their ages, re-determined from literature using these metallicities, and a compilation of [α/Fe] values that are used throughout the paper.

2. Synopsis of previous results

Before starting our present discussion, we summarise the results of our project "Na-O anticorrelation and HB" (Carretta et al. 2006). Up to a few years ago, obtaining adequate high-resolution spectroscopic data sets was painstaking, since stars had to be observed one-by-one. Thanks to the efforts of many researchers, mainly of the Lick-Texas group, spectra of some 200 stars in a dozen GCs were gathered using tens of nights over several years (see the reviews by Kraft 1994; Sneden 2000, and references therein). In the past few years, we used the spectacular data-collecting capability offered by the FLAMES multi-object spectrograph at the ESO VLT to secure spectra for more than 1400 giant stars, distributed over about 12% of all known GCs.

[1] The strong objection made by Renzini (2008) on the outflowing of matter from FRMS being unable to result in clearly separated MS with different – and *discrete* – He content, still applies. However, up to now the only clear cases of several discrete MSs are the very peculiar ω Cen and NGC 2808. Indications for widening of the MS have been obtained for other clusters, such as NGC 104 (Anderson et al. 2009) and NGC 6752, where Milone et al. (2010) also see hint of a split. On the other hand, Renzini (2008) restricts his favourite candidate polluters, AGB stars, to those experiencing only a few episodes of third dredge-up. This might appear too specific and at odds with observed abundances of *s*-process elements in some GCs.

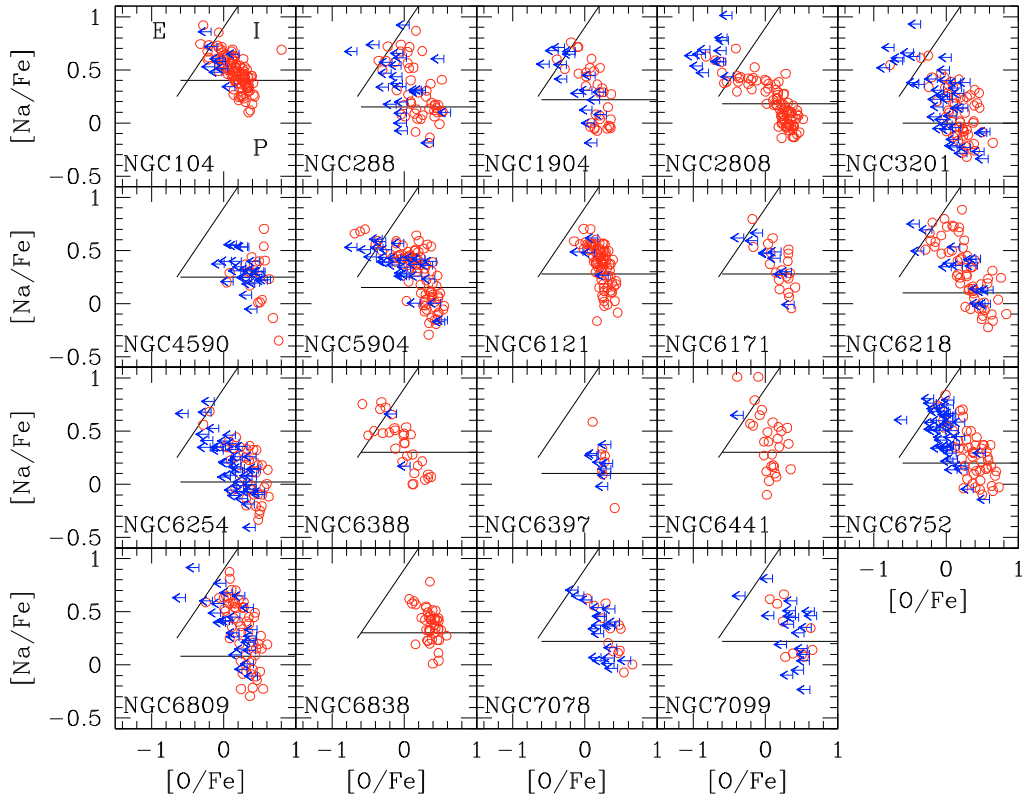

Fig. 1. Summary of the Na-O anticorrelation observed in the 19 GCs of our sample. Arrows indicate upper limits in O abundances. The two lines in each panel separate the primordial component (located in the Na-poor/O-rich region), the Na-rich/O-poor extreme component, and the intermediate component in-between (called P, E, and I, respectively as indicated only in the first panel). See Sect. 2 for details.

With the increase of an order of magnitude in available data, the paradigm has changed. We now understand that the observed anticorrelations are not indicative of "anomalies", rather we are dealing with *the normal chemical evolution of GCs*.

Our survey has already been amply described elsewhere. Results for the first five GCs have been presented in a series of papers (Papers I through VI: Carretta et al. 2006, 2007a,b,c; Gratton et al. 2006, 2007), while the remaining clusters are analysed in Carretta et al. (2009a,b: Paper VII and VIII). In Fig. 1 we show a collage of the Na-O anticorrelations observed in all 19 clusters in our sample. Solid lines separate the primordial, intermediate and extreme populations, whose concept is introduced and defined in Paper VII and recalled briefly below.

We obtained GIRAFFE spectra (at $R \simeq 20\,000$, comprising the Na I 568.2–568.8 nm, 615.4–6.0 nm and [O I] 630 nm lines) of about 100 stars per cluster. At the same time, we also collected UVES spectra (at $R \simeq 40\,000$, covering the 480–680 nm region, and providing information about Mg, Al, and Si, in addition to O and Na) of about 10 stars (on average) per cluster. We homogeneously determined the atmospheric parameters for these stars using visual and near-IR photometry and the relations in Alonso et al. (1999, 2001). We measured Fe, O, and Na abundances for more than 2000 stars (more than 1200 cluster members with *both* O and Na detected), putting together the largest sample of this kind ever collected.

The large number of clusters and stars per cluster allowed us to recognise that the amount of the abundance variations among different clusters is related in a non trivial way to global cluster parameters (Carretta 2006; Carretta et al. 2007a; 2009a, Paper VII: GIRAFFE data; 2009b, Paper VIII: UVES data). The GCs are dominated by the second (polluted) generation of stars, the fraction of primordial stars being roughly correlated with cluster luminosity. The Na-O anticorrelation has not only a different extension, but also a different *shape*, in different clusters, depending on cluster luminosity and metallicity. The Mg-Al anticorrelation is sometimes absent, this occurring in low-luminosity clusters. All these are clear indications that the polluters' properties change from cluster to cluster and that this change is apparently driven by the cluster luminosity and metallicity.

Carretta (2006) suggests using the interquartile range (IQR, the difference between the upper quartile and the lower quartile, see e.g. Tukey 1977) of the [O/Na] ratio as a quantitative measure of the extension of the Na-O anticorrelation. The IQR is useful because it is less influenced by extreme values, because it refers to the range of the middle 50% of the values, and because it is less subject to sampling fluctuations in highly skewed distributions. Statistically robust IQR values require large enough samples of stars. Our project was designed to obtain Na and O abundances for a large number of RGB stars in each cluster, typically 100 stars per cluster, although in some cases only a much smaller sample of stars could be used. The number of stars actually measured in each cluster depends on the richness of population, metallicity, S/N, and in some cases on field-star contamination (such as for the bulge clusters NGC 6388 and NGC 6441 or the disk clusters NGC 6171 and NGC 6838). The smallest sample (16 stars with both Na and O) is for NGC 6397, the largest (115 stars) for 47 Tuc (NGC 104).

In Paper VII we defined three population components in each cluster: the first generation stars and two groups of second generation stars. The lines separating the three components are shown in Fig. 1. The primordial P component includes stars

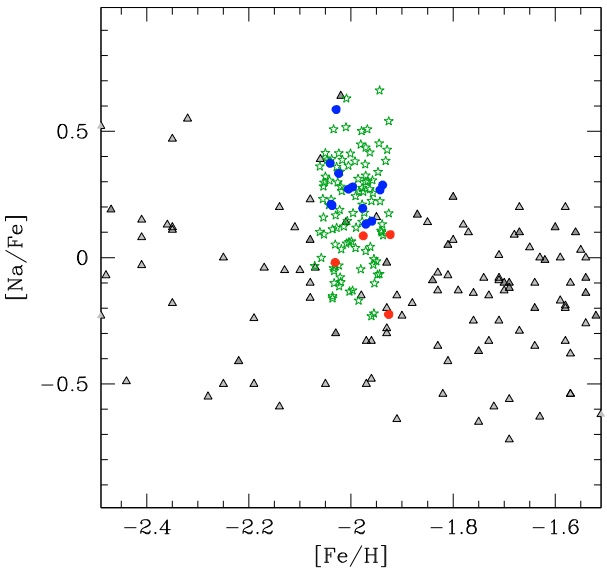

Fig. 2. [Na/Fe] ratios as a function of the metallicity [Fe/H] in a range centred on the average metal abundance of NGC 6397. Filled triangles in grey-tones are field stars from Gratton et al. (2003a) and the compilation by Venn et al. (2004). Filled circles are stars in NGC 6397 with determinations of both O and Na (red: P component, blue: I component). Empty (green) star symbols are stars in NGC 6397 with only Na abundances derived.

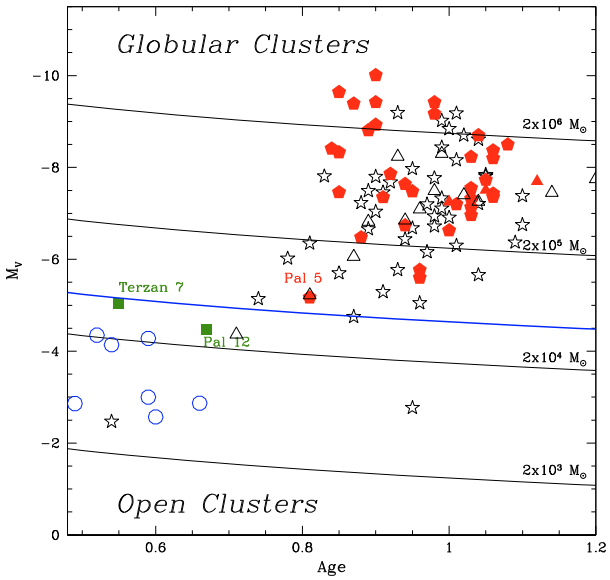

Fig. 3. Relative age parameter vs. absolute magnitude M_V for globular and old open clusters (see Appendix for details). Red filled pentagons and triangles are GCs where Na-O anticorrelation has been observed, in the Milky Way or the LMC, respectively; green squares are clusters that do not show evidence of Na-O anticorrelation, both members of Sagittarius dSph, either of the main body (Terzan 7) or the stream (Pal 12). Open stars and triangles mark clusters for which not enough data is available, in the Milky Way or the LMC respectively. Finally, open circles are old open clusters (data from Lata et al. 2002). Superimposed are lines of constant mass (light solid lines, see Bellazzini et al. 2008a). The heavy blue solid line (at a mass of 4×10^4 $M_\odot$) is the proposed separation between globular and open clusters.

between the minimum [Na/Fe] observed and $[\mathrm{Na/Fe}]_{\mathrm{min}} + 4\sigma$ (see Paper VII). These stars are defined as first-generation objects since they show the same pattern of high O and low Na typical of Galactic field stars of similar metallicity, with the characteristic signature of core-collapse SNe. Since the yields of Na are metallicity-dependent (e.g., Wheeler et al. 1989), the limit for the P component varies as a function of [Fe/H], as is evident in Fig. 1. The separation between the two subcomponents of second-generation stars (the intermediate I stars and the extreme E stars) is somewhat more arbitrary. On the basis of the [O/Na] distributions in our clusters, they were defined in Paper VII as those stars with [O/Na] ratios higher or lower than −0.9 dex, respectively.

Computing the fraction of stars in each component, we found that:

(i) the extreme 2nd generation is not present in all GCs;
(ii) the intermediate 2nd generation constitutes the bulk (50–70%) of stars in a GC;
(iii) the primordial population is present in all GCs (at about the 30% level).

D'Antona and Caloi (2008) use the HB morphology to derive the fraction of stars in two generations in GCs. They made a claim that some clusters (including NGC 6397) could presently host exclusively second-generation stars, since they had completely lost the first-generation ones. However, our abundance analysis, in comparison with field stars, does not support that hypothesis. In Fig. 2 we show the distribution of [Na/Fe] in field stars with metallicity centred on the mean [Fe/H] value for NGC 6397 and our RGB stars in NGC 6397 with both Na and O measurements (Paper VII and Paper VIII), separated in P and I components using our definition. To be very conservative, in Paper VII we attributed only stars with both elements measured to each of the three populations. However, the separation between first and second generation stars (between P and I components) only requires the knowledge of Na abundances. In Fig. 2 we show also the much more numerous stars in NGC 6397 with Na detections. A good fraction of them fall in the region populated by the primordial component and by normal field halo stars, unpolluted by ejecta processed in H-burning. We therefore confirm that, *in all the GCs analysed, a primordial component of first-generation stars is still observable at present*[2].

3. Cluster and parameter selection

3.1. Definition of globular clusters

In this paper we intend to bring together the chemical properties derived from our in-depth study of various stellar populations in GCs with many other global observables. Moreover, we present a scenario for the formation of GCs in the more general context of the relationship between the Milky Way and its satellites. Thus, before entering into the discussion, we recall a few properties of the parent population of GCs that are of direct interest here.

The first point we would like to make concerns the operative definition of *bona fide* GC. The distinction between globular and other clusters (e.g., open clusters) is not well drawn, and it is ambiguous in particular for the populous clusters that are numerous in the Magellanic Clouds. To better clarify this point, we plot in Fig. 3 ages and absolute magnitudes for the clusters listed in the database by Harris (1996, and web updates). This list includes 146 GCs. Seven of these GCs are actually thought to be

[2] While writing this paper, Lind et al. (2009) published the analysis of an extended set of unevolved stars in NGC 6397, and we completed the analysis of turn-off stars in NGC 104 (D'Orazi et al. 2010), where Na abundances show similar variations.

members of the Sagittarius dwarf galaxy (see van den Bergh & Mackey 2004, and references therein). To this sample, we add GCs in other satellites of the Milky Way: 16 GCs in the Large Magellanic Cloud (LMC), 8 in the Small Magellanic Cloud (SMC), and 5 in the Fornax dSph. Data for all these GCs are detailed in the Appendix. Age data are actually available for slightly more than half of the sample. We also add a few old open clusters (NGC 188, NGC 6791, Collinder 261, NGC 1193, Berkeley 31, and Berkeley 39: data from Lata et al. 2002) that fall within the limits of the plot. From this figure, there is a clear overlap between open clusters and objects from the list of GCs at the faint end of the sequence. In (almost) all studied GCs the Na-O anticorrelation has been found. One exception is Terzan 7, where no spread in O abundances has been found in the (only) seven stars observed by Sbordone et al. (2007), and may then be the most massive cluster observed so far without the Na-O anticorrelation. The other one is Pal 12, where Cohen (2004) finds very uniform O and Na abundances, but only for four stars. Finally, there are GCs for which current data are not adequate to state if a Na-O anticorrelation exists or not. Similar data are scarce for open clusters (see Gratton 2007). However, de Silva et al. (2009) have compiled data for various old open clusters, finding no evidence of an Na-O anticorrelation, and Martell & Smith (2009) did not find any evidence of CN variation among giants in three open clusters (including NGC 188). This diagram indicates that the Na-O and related anticorrelations have been observed in all old clusters with $M_V < -5.1$ (which roughly corresponds to a mass of $\sim 4\times10^4$ $M_\odot$ for old populations), including the vast majority of Galactic GCs, and almost all the objects with a relative age parameter >0.8. *We then propose to identify the GCs with those clusters where there is an Na-O anticorrelation*. As we see in Sect. 4.1, this identification corresponds to a formation scenario that clearly separates GCs from other clusters. Operatively, we might also define GCs either as the old clusters (age over 5 Gyr) with an $M_V < -5.1$ or those with relative age parameter >0.8. These definitions essentially include the same list of objects, at least in the Milky Way and its satellites.

At the other mass limit for the GC population, the similarity between GCs and nuclei of dwarf galaxies has been pointed out by many authors (see e.g. Freeman 1990; Böker 2008; Georgiev et al. 2009). Those nuclei or nuclear star clusters of dwarf galaxies that can be studied in close detail (such as M 54 for the Sagittarius galaxy) essentially share the full pattern of properties with GCs (see e.g. Bellazzini et al. 2008b; Georgiev et al. 2009; Carretta et al. 2010), although they may have wide spreads in Fe abundances, not observed in GCs. This occurrence suggests that also ω Cen was (in) the nucleus of a galaxy in the past.

3.2. Our sample of GCs

Ideally, we should have derived detailed chemical data for the whole parent population. However, this would have required too much observing time, so we analysed only a representative subset of clusters (representing about 12% of the total sample). The selection procedure was as follows. We started from the complete sample of Galactic GCs, as listed by Harris (1996). We then divided clusters into different groups, according to the morphology of the HB. For each group, we selected the two-four rich ($M_V < -5$) clusters, accessible from Paranal ($\delta < +20°$), with the smallest apparent distance modulus; however, we did not consider some clusters that have quite large differential reddening (like M 22: Ivans et al. 2004[3]). The selected clusters were: red HB clusters: NGC 104=47 Tuc, NGC 6838=M 71, NGC 6171=M 107; Oosterhoff I clusters: NGC 6121=M 4, NGC 3201, NGC 5904=M 5; blue HB clusters: NGC 6752, NGC 6218=M 12, NGC 6254=M 10, NGC 288, NGC 1904=M 79; clusters with blue, short HB's: NGC 6397, NGC 6809=M 55; Oosterhoff II clusters: NGC 7099=M 30, NGC 4590=M 68, NGC 7078=M 15; clusters with very extended/bimodal distribution of stars on the HB: NGC 2808, NGC 6441, NGC 6388. As a result, within each different class of HB morphology, the sample is essentially distance-limited. On the other hand, this is not true for the whole sample, because the adopted limits depend on the morphological classes and reddening (so that clusters projected close to the Galactic plane are under-represented). However, for most classes of HBs, the limit is quite uniform at about $(m - M)_V < 14.5-15.5$, which is ~10 kpc from the Sun. We needed to sample a larger volume ($(m - M)_V < 16.5$) to include GCs with very extended/bimodal distribution of stars on the HB, since these clusters are rare. These choices mean that GCs with very extended blue HB are over-represented in our sample (42% of the total).

3.3. The Galactic GC sample

To correctly explore the relations between the chemistry of different stellar generations and global GC properties, it is important to assess to what cluster population our programme GCs belong. Zinn (1985) demonstrated that Milky Way GCs can be divided into two main groups: disk (or bulge) GCs and halo GCs. This separation was done according to the metal abundance alone (with the limit at [Fe/H] = −0.8 dex). These two groups correspond to the main peaks of the metallicity distribution of GCs, but they can also be clearly distinguished from other properties (location in the Galaxy, kinematics, etc.). According to Searle & Zinn (1978), halo GCs result from the evolution of individual fragments, while disk clusters likely formed within the dissipational collapse. This distinction is thus likely to play an important rôle in defining the characteristics of GCs and, in particular, of their primordial population.

Further refinements (e.g., van den Bergh & Mackey 2004; Lee et al. 2007) along Zinn's line of thought were done by using the HB morphology, which is, however, one of the features of GCs we intend to explain. In the following, therefore, we adopt a combination of location in the Galaxy and kinematics criteria to separate disk clusters from the halo ones[4]. Full details are given in the Appendix. Briefly, using the Harris (1996) catalogue, we first classified as outer halo GCs the ones currently located at distances greater than 15 kpc (Carollo et al. 2008) from the Galactic centre, and clusters with Galactocentric distance less than 3.5 kpc were instead considered as bulge GCs. To separate the inner halo clusters from the disk ones, we used the rotational velocity around the Galactic centre by Dinescu et al. (1999) and Casetti-Dinescu et al. (2007) whenever possible. When this information was not available, we used the differences between the observed radial velocity (corrected to the LSR) and the one expected from the Galactic rotation curve (see Clemens 1985). In

[3] A chemical analysis similar to ours has been performed in M 22 by Marino et al. (2009). This data, kindly given to us before publication, nicely fit in our relations. However, we do not include it in the present analysis because it is not strictly homogeneous.

[4] Similarly, Pritzl et al. (2005) adopted kinematics to assign GCs to various Galactic components; however they were able to do so only for 29 of the 45 GCs they studied.

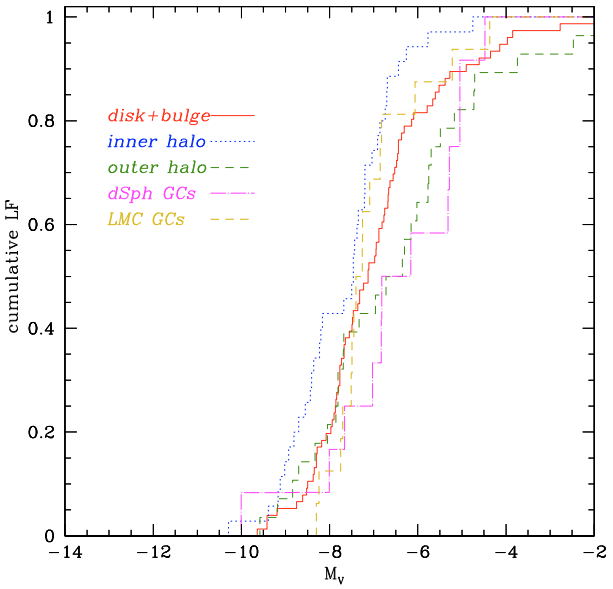

Fig. 4. Cumulative luminosity functions of different groups of Galactic GCs (from the Harris 1996 catalogue) according to our present classification criteria and of GCs in dSphs (from van den Bergh and Mackey 2004; see Appendix for references on Fornax an LMC clusters). The red solid line indicates disk/bulge clusters, the blue dotted line the inner halo clusters, the dashed green line clusters in the outer halo, magenta dashed-dotted line is for clusters in dSphs, and the green-gold long dashed line for GCs in LMC.

the Appendix we provide the disk/inner halo/outer halo classification for each cluster listed in the Harris catalogue. Finally, we consider GCs in the LMC and SMC and in dSphs (Sagittarius and Fornax) as separate groups.

The procedure for selecting the programme sample, described in Sect. 3.2, results in a potential selection bias as a function of the distance. This shows up in a correlation between a cluster's present-day mass (as represented by the proxy of cluster total absolute visual magnitude, M_V) and distance modulus, so that in our sample more massive GCs are typically the most distant ones. This correlation is at odds with the total sample of GCs in the Harris (1996) catalogue. However, since all programme GCs but one (NGC 1904, with $R_{GC} = 18.8$ kpc) are within 15 kpc of the Galactic centre, they belong either to the disk or to the inner halo. Within this subsample, there is a correlation of M_V with Galactocentric distance similar to what was noticed in our sample. We thus assume that our sample is representative of the properties of the disk and inner halo (but not of the outer halo) GCs and neglect the possible bias with luminosity.

Other properties of the parent population of Galactic GCs relevant to our discussion are the masses (luminosities) and the metallicities of the disk and inner halo GCs. These are two of the main parameters driving most of the observed properties of GCs, as we confirm later, so they are worth a few more words.

Inner and outer halo clusters have clearly distinct luminosity functions (LF), as illustrated by Fig. 4. Small clusters ($M_V > -6$) only exist in the outer halo, where they make up half of the total. A Kolmogorov-Smirnov test returns a 1% probability that inner and outer halo LFs were extracted from the same population. Of course, this difference can be at least in part attributed to the destruction mechanisms, which are more efficient for clusters closer to the centre of the Galaxy. However, other mechanisms can also be considered. In fact, all young clusters (age parameter <0.8) reside in the outer halo, and they are allfaint ($M_V > -6.5$), overlapping open clusters in the M_V/age distribution (Fig. 3). If we limit ourselves to old clusters (age parameter >0.82, essentially adopting the same definition of GC considered in Sect. 3.1), there is no clear difference between the LF of inner halo or disk and that of outer halo clusters (Kolmogorov-Smirnov tests applied to the distributions of GCs having age parameter result into a significance of 16 and 32%, respectively).

The comparison between the LFs of disk and inner halo GCs is also worth more attention. Again, we naively expected that destruction mechanisms would be more effective for disk clusters than for the inner halo ones. In this case, the LF for inner halo clusters should have a fraction of low-mass clusters intermediate between those observed in the outer halo and in the disk. However, while only 19% (4%) of the inner halo GCs have $M_V > -7$ ($M_V > -6$), this percentage is 41% (15%) for disk clusters. There are very few inner halo counterparts of the very frequent small disk clusters like M 71 and NGC 6397. Since such clusters are more easily destroyed in the disk than in the inner halo, this suggests a different original mass distribution between the disk and the inner halo (see also Fraix-Burnet et al. 2009, who attempted a multi-parametric classification of GCs, different from ours and leading to different conclusions about the properties of the different cluster populations, see the Appendix for further details).

All this suggests that the main difference between disk, inner, and outer halo clusters might be related to their formation (absence of young, small clusters in the inner halo) more than to the destruction efficiency, which is however very important for small clusters. This goes against a diffuse opinion, i.e., that we are now seeing only those GCs that occupied the survival zone of parameters; however, the notion that GCs can be formed only in a limited range of parameters is not new, as seen in Caputo & Castellani (1984).

It is also interesting to note that the luminosity function of the outer halo GCs is similar to that of GCs in dSphs (see Fig. 4): a Kolmogorov-Smirnov test gives a chance (73%) that they were drawn from the same parent population. This might depend on the fact that clusters in the outer halo and dSph shared similar environments at birth.

Disk and halo GCs also differ in other important characteristics. Obviously, the inner halo/outer halo GCs are on average more metal poor than the disk ones (see Appendix). Furthermore, they seem to obey different age metallicity relations: metallicity increased slower in the inner halo than in the disk, and even slower in the outer halo, see Fig. 5. The age estimates were obtained as described in the Appendix. Practically all disk/bulge GCs with [Fe/H]< -1 are very old, while most of the inner halo GCs of intermediate metallicity ($-2 <$ [Fe/H] < -1) have relative ages in the range 0.8–0.9; i.e., they are about 2 Gyr younger than disk GCs with the same metallicity. If the age/metallicity calibration is correct, after 2 Gyr from the Big Bang, the central region of the Milky Way was enriched to [Fe/H] ~ -0.4 (and [α/H]$\sim$ 0), while the inner halo metallicity was still very low[5].

[5] This does not mean that the pace of evolution was uniformly slower in the halo than in the disk. It is indeed possible that star formation (and chemical evolution) in the halo actually occurred in bursts separated by long quiescent phases, while it was characterised by prolonged phases at a relatively low level in the disk. This might lead to the paradoxical situation that stars in the halo have a chemical composition more appropriate to faster star formation than those in the disk, although the former might actually be younger. We come back to this point in the next section.

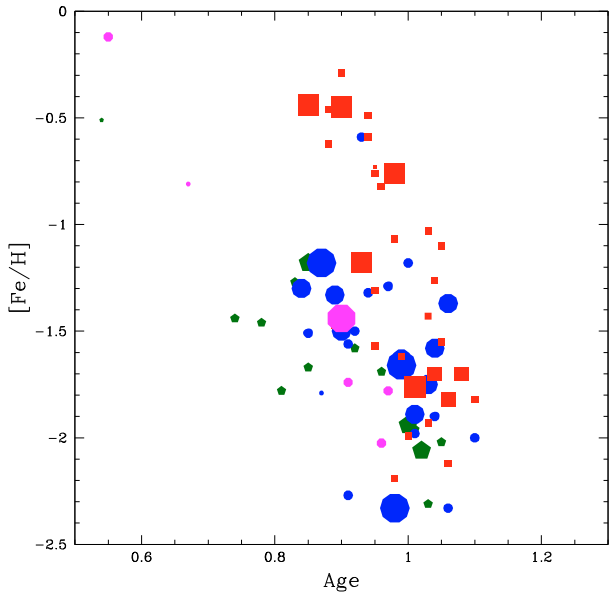

Fig. 5. Age-metallicity relation for different groups of GCs: outer halo clusters (green pentagons), inner halo clusters (blue circles), disk/bulge clusters (red squares). Magenta circles are GCs associated to dSphs. Different symbol sizes are used for clusters of different luminosity.

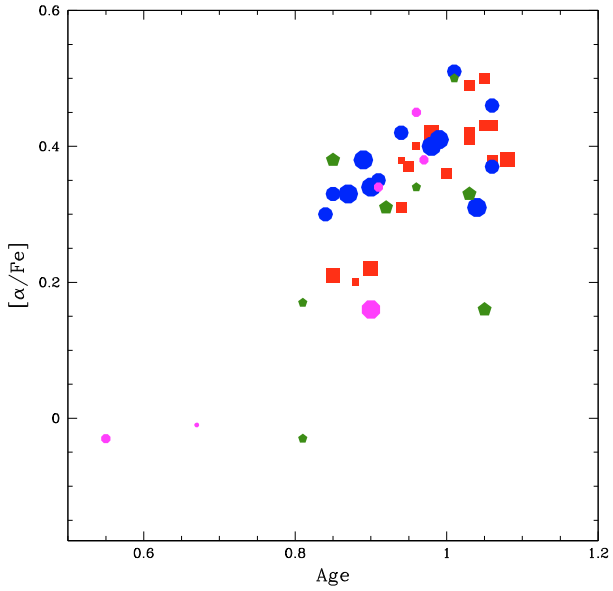

Fig. 6. Relation between age and excess of α-elements for different groups of GCs (the meaning of symbols is as in Fig. 5). [α/Fe] values come from our compilation of literature data (see Appendix). Different symbol sizes are used for clusters of different luminosities.

Finally, disk and inner halo GCs may differ in their element-to-element abundance ratios, as suggested by the analysis by Lee & Carney (2002). In part, this can be attributed to an age effect (see Fig. 6); however, age cannot be the only explanation. This is shown by the close comparison between M 4 and M 5 (NGC 6121 and NGC 5904), performed by Ivans et al. (2001), which is fully confirmed by our analysis (Carretta et al. 2009b). These GCs are both inner-halo clusters according to our classification, although M 5 has much more extreme kinematics, and it is also likely younger by more than 1 Gyr. M 5 has a smaller excess of α-elements and also seems to be deficient in nuclei produced by s-process nucleosynthesys (Ivans et al. 2001; Yong et al. 2008). If confirmed, these two facts might at first look contradictory, since a lower excess of α-elements is usually attributed to a prolonged star formation, allowing significant contribution by type Ia SNe. However, such a long phase of star formation should also allow the contribution by the intermediate and low-mass AGB stars, which efficiently produce s-elements. In the next sections, we re-examine this point using our extensive database and find a solution to this conundrum.

3.4. Cluster parameters considered in the analysis

Our choice was driven by the aim of sampling the full parameter space of GCs and to derive relations between the properties of different stellar generations in GCs and global parameters. Table 1 lists the 19 GCs in our programme set and gives structural and orbital parameters taken from literature. We considered the following parameters, mostly from Harris (1996):

- the apparent visual distance modulus, $(m - M)_V$;
- the reddening, $E(B - V)$;
- the Galactocentric distance, R_{GC};
- the total absolute visual magnitude, M_V;
- the HB ratio, HBR, that is the fraction of blue and red HB stars over the total, as $(B - R)/(B + V + R)$;
- the metallicity, [Fe/H] from our Paper VIII;
- the cluster ellipticity, *ell*;
- the concentration, c;
- the tidal radius, r_t (in pc, from Mackey & van den Bergh 2005);
- the half light radius, r_h (in pc, from Mackey & van den Bergh 2005).

We considered the following parameters related to the Galactic orbit (from Dinescu et al. 1999; Casetti-Dinescu et al. 2007):

- the total energy of orbit, E_{tot};
- the period of the Galactic orbit, P;
- the apogalactic distance, R_{apo};
- the perigalactic distance, R_{per};
- the maximum distance from the plan, z_{max};
- the eccentricity of the orbit, *ecc*;
- the inclination angle of the orbit, ψ;
- the rotational velocity, Θ.

These orbital parameters are mean values averaged over a large number of orbits. As a result, they represent a way to gain knowledge of the birthplace of clusters and of the conditions existing at their formation epoch, and where most of their lifetime is spent in the Galaxy. Instantaneous quantities, such as the present Galactocentric distance of a GC, may be much less informative. Unfortunately, no orbital parameters have been determined yet for the two most massive clusters in our sample, NGC 6388 and NGC 6441. In addition, we considered the relative age parameter, mostly re-determined from Marin-Franch et al. (2009) and De Angeli et al. (2005) as described in the Appendix.

In Table 2 we report a few of the parameters derived by our works, related to the chemistry of first and second generation stars in GCs and their link with primordial abundances existing at the epoch of their formation. Other parameters derived, but not listed, in Papers VII and VIII are also given in this table.

Among these, we considered parameters related to the chemistry of first generation stars:

- the maximum O abundance, $[O/Fe]_{max}$;
- the minimum Na abundance, $[Na/Fe]_{min}$;

Table 1. Properties of the 19 GCs in our sample.

NGC	Other	$(m-M)_V$[1]	$E(B-V)$[1]	R_{GC}[1]	Z[1]	$M_{V,tot}$[1]	HBR[1]	[Fe/H][1]	ell[1]	c[1]	r_h[1]	r_t[1]
104	47Tuc	13.32	0.04	7.4	–3.2	–9.42	–0.99	–0.768	0.09	2.03	2.79	42.86
288		14.64	0.03	12.0	–8.8	–6.74	0.98	–1.305		0.96	2.22	12.94
1904	M79	15.53	0.01	18.8	–6.3	–7.86	0.89	–1.579	0.01	1.72	0.80	8.34
2808		15.59	0.22	11.1	–1.9	–9.39	–0.49	–1.151	0.12	1.77	0.76	15.55
3201		14.17	0.23	8.9	0.8	–7.46	0.08	–1.512	0.12	1.30	2.68	28.45
4590	M68	15.14	0.05	10.1	6.0	–7.35	0.17	–2.265	0.05	1.64	1.55	30.34
5904	M5	14.41	0.03	6.2	5.4	–8.81	0.31	–1.340	0.14	1.83	2.11	28.40
6121	M4	12.78	0.36	5.9	0.6	–7.20	–0.06	–1.168	0.00	1.59	3.65	32.49
6171	M107	15.01	0.33	3.3	2.5	–7.13	–0.73	–1.033	0.02	1.51	2.70	17.44
6218	M12	13.97	0.19	4.5	2.2	–7.32	0.97	–1.330	0.04	1.39	2.16	17.60
6254	M10	14.03	0.28	4.6	1.7	–7.48	0.98	–1.575	0.00	1.40	1.81	21.48
6388		16.49	0.37	3.2	–1.2	–9.42	–0.65	–0.441	0.01	1.70	0.67	6.21
6397		12.31	0.18	6.0	–0.5	–6.63	0.98	–1.988	0.07	2.50	2.33	15.81
6441		16.33	0.47	3.9	–1.0	–9.64	–0.76	–0.430	0.02	1.85	0.64	8.00
6752		13.08	0.04	5.2	–1.7	–7.73	1.00	–1.555	0.04	2.50	2.34	55.34
6809	M55	13.82	0.08	3.9	–2.1	–7.55	0.87	–1.934	0.02	0.76	2.89	16.28
6838	M71	13.70	0.25	6.7	–0.3	–5.60	–1.00	–0.832	0.00	1.15	1.65	8.96
7078	M15	15.31	0.10	10.4	–4.7	–9.17	0.67	–2.320	0.05	2.50	1.06	21.50
7099	M30	14.57	0.03	7.1	–5.9	–7.43	0.89	–2.344	0.01	2.50	1.15	18.34

NGC	other	E_{tot}[2]	P[2]	R_{apo}[2]	R_{per}[2]	z_{max}[2]	ecc[2]	ψ[2]	Θ	age[3]
104	47Tuc	–872	190	7.3	5.2	3.1	0.17	29	161	0.95
288		–787	224	11.2	1.7	5.8	0.74	44	–27	0.90
1904	M79	–526	388	19.9	4.2	6.2	0.65	28	83	0.89
2808		–770	240	12.3	2.6	3.8	0.65	18	74	0.83
3201		–430	461	22.1	9.0	5.1	0.42	18	–301	0.82
4590	M68	–396	504	24.4	8.6	9.1	0.48	30	300	0.94
5904	M5	–289	722	35.4	2.5	18.3	0.87	33	115	0.85
6121	M4	–1121	116	5.9	0.6	1.5	0.80	23	24	0.97
6171	M107	–1198	87	3.5	2.3	2.1	0.21	44	151	0.99
6218	M12	–1063	125	5.3	2.6	2.3	0.34	33	130	0.99
6254	M10	–1053	128	4.9	3.4	2.4	0.19	33	149	0.92
6388										0.87
6397		–1017	143	6.3	3.1	1.5	0.34	18	133	0.99
6441										0.83
6752		–977	156	5.6	4.8	1.6	0.08	18	199	1.02
6809	M55	–1038	122	5.8	1.9	3.7	0.51	56	55	1.02
6838	M71	–957	165	6.7	4.8	0.3	0.17	3	180	0.94
7078	M15	–752	242	10.3	5.4	4.9	0.32	36	128	1.01
7099	M30	–937	159	6.9	3.0	4.4	0.39	52	–1.4	1.08

Notes. [(1)] Global parameters, from Harris (1996), except [Fe/H], which is from UVES spectra (Paper VIII) and the HBR for NGC 6388, NGC 6441 calculated from Busso et al. (2007); [(2)] orbital parameters, from Dinescu et al. (1999), Casetti-Dinescu et al. (2007). Units are: 10^2 km^2 s^{-2} (E_{tot}), 10^6 yr (P), kpc (R_{apo}, R_{per}, z_{max}), degrees (ψ), km s^{-1} (Θ); [(3)] relative age (see Appendix).

- the maximum Mg abundance, $[Mg/Fe]_{max}$;
- the minimum Al abundance, $[Al/Fe]_{min}$;
- the minimum Si abundance, $[Si/Fe]_{min}$;
- the total Mg+Al+Si content, where the average is done in number, not in logarithm, [(Mg+Al+Si)/Fe];
- the overabundance of α-elements, [α/Fe], as given by the average of $[Mg/Fe]_{max}$, $[Si/Fe]_{min}$, and [Ca/Fe] (see Sect. 4.2.1 for an explanation of the choice).

Coupled with [Fe/H], these parameters essentially describe the starting composition of the proto-GCs. The elements considered here are mainly produced by core-collapse SNe, with some contribution by thermonuclear SNe for what concerns Fe (and marginally Si). The sum Mg+Al+Si essentially describes the primordial abundance of elements with $24 < A < 28$ for two reasons. First, this quantity does not differ between different stellar generations in a cluster. As an example, in NGC 2808, the average value of the ratio [(Mg+Al+Si)/Fe] is $+0.29 \pm 0.01$ dex (rms = 0.03 dex) for the 9 stars in the P and I components and $+0.28 \pm 0.02$ dex (rms = 0.04 dex) for the three stars with subsolar Mg values, belonging to the E component (see Paper VIII, Al was measured only on UVES spectra). Second, the only way to get significant modifications of this primordial ratio is to produce the dominant species ^{24}Mg or ^{28}Si from SN nucleosynthesis. In the following, we therefore adopt this ratio essentially as another indicator of the α-element level in a cluster[6].

[6] Of course, Al is not an α-element. However, in the primordial populations, Al abundance is always negligible with respect to that of Mg and Si; therefore, for these stars the sum of Mg+Al+Si is essentially the sum of Mg+Si. Within the GC, when some stars are very rich in Al, this comes from p-captures on ^{24}Mg, ^{25}Mg, ^{26}Mg. This Al results then from material originally produced as α-rich, and the total of Mg+Al+Si is conserved throughout these reactions. For this reason, we may use this sum as an indicator of the abundance of the α-elements.

Table 2. Quantities for the same GCs, derived by our works.

NGC	$\log T_{\rm eff}^{\rm max}$ (HB)	IQR[Na/O][1]	P[2]	I[2]	E[2]	$\langle[\alpha/{\rm Fe}]\rangle$[3]	[(Mg+Al+Si) /Fe][6]	$[{\rm Mg/Fe}]_{\rm max}^{6}$	$[{\rm Mg/Fe}]_{\rm min}^{6}$	$[{\rm Si/Fe}]_{\rm min}^{6}$	$[{\rm Si/Fe}]_{\rm max}^{6}$
104	3.756[4]	0.472	27	69	4	0.42	0.46	0.60	+0.47	0.35	0.43
288	4.221[5]	0.776	33	61	6	0.42	0.41	0.55	+0.41	0.30	0.41
1904	4.352[4]	0.759	40	50	10	0.31	0.31	0.40	+0.16	0.25	0.34
2808	4.568[4]	0.999	50	32	18	0.33	0.29	0.42	−0.30	0.22	0.38
3201	4.079[4]	0.634	35	56	9	0.33	0.32	0.45	+0.27	0.25	0.41
4590	4.041[4]	0.372	40	60	0	0.35	0.40	0.48	+0.28	0.30	0.48
5904	4.176[4]	0.741	27	66	7	0.38	0.36	0.55	+0.31	0.21	0.39
6121	3.968[5]	0.373	30	70	0	0.51	0.54	0.65	+0.50	0.45	0.64
6171	3.875[4]	0.522	33	60	7	0.49	0.53	0.60	+0.46	0.45	0.63
6218	4.217[4]	0.863	24	73	3	0.41	0.43	0.60	+0.46	0.22	0.43
6254	4.400[5]	0.565	38	60	2	0.37	0.37	0.58	+0.33	0.18	0.36
6388	4.255[4]	0.795	41	41	19	0.22	0.30	0.40	+0.16	0.20	0.46
6397	3.978[4]	0.274	25	75	0	0.36		0.55	+0.40	0.25	0.43
6441	4.230[4]	0.660	38	48	14	0.21	0.34	0.45	+0.20	0.15	0.45
6752	4.471[5]	0.772	27	71	2	0.43	0.44	0.60	+0.36	0.28	0.49
6809	4.153[5]	0.725	20	77	2	0.42	0.43	0.60	+0.18	0.30	0.51
6838	3.763[4]	0.257	28	72	0	0.40	0.44	0.60	+0.39	0.30	0.51
7078	4.477[4]	0.501	39	61	0	0.40	0.46	0.68	−0.01	0.28	0.60
7099	4.079[4]	0.607	41	55	3	0.37	0.44	0.60	+0.44	0.20	0.45

Notes. [(1)] IQR([Na/O]) comprises stars with GIRAFFE and UVES data; [(2)] P, I, E are fraction of stars of Primordial, Intermediate, Extreme populations from Paper VII; [(3)] $[\alpha/{\rm Fe}]$ is the average of $[{\rm Mg/Fe}]_{\rm max}$, $[{\rm Si/Fe}]_{\rm min}$ and [Ca/Fe]; [(4)] $\log T_{\rm eff}^{\rm max}$(HB) taken from Recio-Blanco et al. (2006); [(5)] $\log T_{\rm eff}^{\rm max}$(HB) derived in the present work (see Sect. 5.2); [(6)] from Paper VIII.

Parameters related to the internal chemical evolution within the clusters are

- the minimum O abundance, $[{\rm O/Fe}]_{\rm min}$;
- the maximum Na abundance, $[{\rm Na/Fe}]_{\rm max}$;
- the minimum Mg abundance, $[{\rm Mg/Fe}]_{\rm min}$;
- the maximum Al abundance, $[{\rm Al/Fe}]_{\rm max}$;
- the maximum Si abundance, $[{\rm Si/Fe}]_{\rm max}$;
- the relative fraction of stars in primordial (P), intermediate (I), and extreme (E) groups;
- the interquartile range of the [O/Na] ratio, IQR[O/Na].

Minimum and maximum abundances of different elements were estimated as discussed in Papers VII and VIII, using a dilution model that reproduces the run of the observed Na-O, Mg-Al and Mg-Si anticorrelations in GCs.

Finally, to explore the connection between chemical patterns of light elements, He abundances, and HB morphology we considered the maximum temperature $\log T_{\rm eff}^{\rm max}$(HB) reached on the blue tail of the HB (taken by Recio-Blanco et al. 2006 or computed by us for programme clusters not listed in that study).

4. First generation stars, primordial abundances, and scenarios for cluster formation

The chemical pattern in first-generation GC stars is strictly related to the pre-enrichment established in the precursors of GCs, an issue for which we only have, at the very best, indirect evidence. In this section we discuss what evidence can be obtained from our data on the scenario of formation of GCs.

4.1. The masses of proto-GCs and the relation between the primordial population of GCs and the field

The scenario we are devising assumes that practically *all* GCs started their evolution as large cosmological fragments. To put cluster formation in a broader context, we try to establish the order of magnitude of the mass involved in cluster formation and discuss the possible link between GCs and field stars. Using different lines of thought, several authors (Larson 1987; Suntzeff & Kraft 1996; Decressin et al. 2008; D'Ercole et al. 2008) have suggested that present-day GCs are only a fraction (likely small) of the original structures where they originated. Large amounts of mass should be lost by proto-clusters during the early phases of formation (a few 10^7 yr), mainly for two reasons. First, the efficiency of transformation of gas into stars is unlikely to be larger than 50%, and it is more likely between 20 to 40% (Parmentier et al. 2008). The interaction with the high-velocity winds from massive stars and by their SN explosions expels the residual gas from the cluster and ram pressure probably contributes to the loss. Second, massive stars lose a large fraction of their mass before they become collapsed remnants. Several tens of per cent of the initial mass of the cluster may be lost by these stars, depending on the stellar initial mass function (IMF).

Owing to this huge mass loss, the clusters experience a violent relaxation (Lynden-Bell 1967), with a considerable expansion – beyond the tidal radius – and ensuing loss of stars. As shown by Baumgardt et al. (2008), the gas loss may destroy as much as 95% of the clusters, and this is a basic difficulty in forming bound star clusters. Only clusters with very high mass and initial concentration may survive. Clusters with a relatively flat stellar mass spectrum would be disrupted by this mass loss (Chernoff & Weinberg 1990). A bell-shaped cluster mass function, not too dissimilar to the observed one, can be reproduced by a proper tuning of parameters (efficiency of star formation, initial central concentration, original mass distribution, initial stellar mass function: see e.g., Parmentier & Gilmore 2007; Kroupa & Boily 2002). However, given the uncertainties existing in these parameters, the exact fraction of primordial mass lost by the proto-GCs is not determined well.

On the other hand, it is currently fully assessed that the second-generation stars (that presently make up some 2/3 of the

stars of a typical GC, see Paper VII) should have formed from the ejecta of only a fraction of the first-generation stars, that actually coincide with the primordial component in GCs (Prantzos & Charbonnel 2006). To explain the present GC mass, we should then assume: (i) that the clusters originally had many more stars in the primordial component than we currently observe; and ii) that they selectively lost most of their primordial population, while retaining most of the second-generation stars. D'Ercole et al. (2008) presented a viable hydrodynamical scenario that meets both these requirements. In this scenario, a cooling flow channels the material, ejected as low-velocity winds from massive AGB stars of the first-generation, to the centre of the potential well. The first-generation stars were at the epoch expanding due to the violent relaxation caused by the mechanisms cited above. Given their very different kinematics, first and second generation stars are lost by the cluster at very different rates (at least in the early phases), leaving a kinematically cool, compact cluster dominated by second-generation stars. This selective star loss may continue until two-body relaxation redistributes energy among stars. This takes a few relaxation times, that is, some 10^8–10^9 yr in typical GCs. After that, the effect could even be reversed if He-rich second-generation stars are less massive than first-generation ones (see D'Ercole et al. 2008; Decressin et al. 2008).

We may roughly estimate the initial mass of the primordial population needed to provide enough mass for the second generation by the following procedure:

(i) We assume an IMF for both the first and second generations. For simplicity; we assumed that the two populations have the same IMF. We considered both power-law (like the Salpeter 1955 one) and the Miller & Scalo (1979, MS) IMF's. As often done, in the first case we integrated the IMF over the range 0.2–50 $M_\odot$[7], while in the second case we considered the range 0.1–100 $M_\odot$.

(ii) We also assumed an initial-final mass relation. In practice, we assumed a linear relation, with final mass ranging from 0.54 to 1.24 $M_\odot$, over the mass range from 0.9 to 8 $M_\odot$ (Ferrario et al. 2005). A second linear relation with final mass ranging from 1.4 to 5 $M_\odot$ was assumed for the mass range from 8 to 100 $M_\odot$. The latter relation is not critical, since massive stars lose most of their mass.

(iii) We assume that the second generation is made of the ejecta of stars in the mass range between $M_{\rm min}$ and $M_{\rm max}$. The adopted ranges were 4–8 $M_\odot$ for the massive AGB scenario and 12–50 $M_\odot$ for the FRMS. Second-generation stars likely result from a dilution of these ejecta with some material with the original cluster composition. A typical value for this dilution is that half of the material from which second-generation stars formed was polluted, and half had the original composition. The origin of this diluting material is likely to be pristine gas (not included into primordial stars, see Prantzos & Charbonnel 2006).

(iv) We finally assume that none of the second generation stars is lost, while a large fraction of the primordial generation stars evaporate from the clusters. Of course, this is a schematic representation.

With these assumptions, the original population ratio between first and second-generation stars in GCs depends on the assumed IMF, as detailed in Table 3. To reproduce the observed ratio between first and second generation stars (33%/66% = 0.5), the original cluster population should have been much larger than the current one. If the polluters were massive AGB stars, larger by roughly an order of magnitude if a Salpeter (1955) IMF is adopted (the same result was obtained by Prantzos & Charbonnel 2006), and by a lower value (about 7) if the Miller & Scalo (1979) IMF is adopted. If this is correct, we may expect to find many stars in the field coming from this primordial population. According to Table 3 and in the extreme hypothesis that all field stars formed in the same episode that led to the formation of present-day GCs, the ratio between field and GC stars ranges between 4 and 10 if the polluters were massive AGB stars. It may be lower by more than a factor of 2 if the polluters were instead FRMS. Of course, this is likely an underestimate, since we neglected various factors. Also, second-generation stars may be lost by GCs; low-mass stars are selectively lost; and a significant fraction – even the majority – of field stars may have formed in smaller episodes of star formation.

We conclude that, during the early epochs of dynamical evolution, a proto-GC should have lost ~90% of its primordial stellar population. A GC of a few 10^7 yrs old should have then appeared as a compact cluster immersed in a much larger loose association of stars and an even more extended expanding cloud of gas. Objects with these characteristics have been observed in galaxies with very active star formation (see e.g. Vinko et al. 2009).

Observational constraints to the ratio between first and second generation stars may be obtained by comparing the number of stars within the GCs with that of the related field population. To have an estimate of the amount of mass lost by GCs during their evolution, we may use the peculiar composition of GC

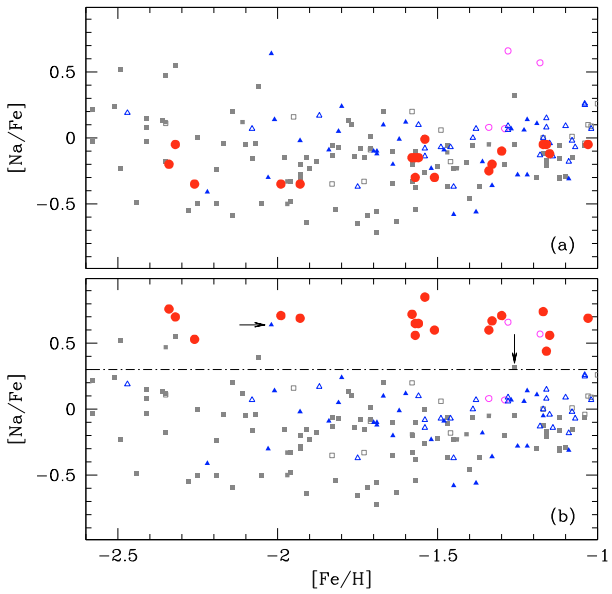

Fig. 7. Comparison of [Na/Fe] values between field and GC stars as a function of metallicity. In both panels the filled red circles are for our sample of GCs, indicating $[Na/Fe]_{min}$ in panel **a)** and $[Na/Fe]_{max}$ in panel **b)**, with the dot-dashed line at [Na/Fe] = 0.3 (see text). [Na/Fe] ratios for field stars are the same in both panels and are taken from Fulbright et al. (2007: magenta open circles, bulge stars), Gratton et al. (2003a: blue filled triangles for accreted and open triangles for dissipation components, respectively), and Venn et al. (2004: grey filled squares for halo and open squares for thick disk stars, respectively). Small arrows in panel **b)** indicate the two field stars that seem genuine second generation stars evaporated from GCs (see text).

[7] Had we integrated the IMF over the range 0.1–50 $M_\odot$, which clearly leads to overestimating the fraction of low-mass stars (see Chabrier 2003), the values in Cols. 5–7 of Table 3 should have been increased by ~50%.

Table 3. Original/final mass of GCs required to produce the observed ratios between number of stars in first and second generations.

Prim/2nd gen Current	IMF Slope	M_{min}	M_{max}	Prim/2nd gen Original	Original/Current	Field/GCs
(1)	(2)	(3)	(4)	(5)	(6)	(7)
Massive AGB stars (HBB)						
0.5	1.35	4	8	11.1	7.4	6.4
0.5	1.85	4	8	9.7	6.5	5.5
0.5	2.35	4	8	15.8	10.6	9.6
0.5	MS	4	8	7.3	4.9	3.9
Fast rotating massive stars						
0.5	1.35	12	50	1.8	1.2	0.2
0.5	1.85	12	50	3.3	2.2	1.2
0.5	2.35	12	50	11.2	7.5	6.5
0.5	MS	12	50	3.0	2.3	1.3

Notes. [(1)] Current ratio between first and second generation stars; [(2)] slope α of the IMF ($N(M) = M^{-\alpha}$; Salpeter (1955) IMF has $\alpha = 2.35$; MS means that the IMF by Miller & Scalo (1979) is adopted; [(3)] Minimum polluter mass (in $M_{\odot}$); [(4)] maximum polluter mass (in $M_{\odot}$); [(5)] original ratio between first and second generation stars; [(6)] ratio between the number of low-mass stars in the proto-cluster and in the current GC; [(7)] current ratio of field stars (=primordial population lost by the cluster) and of GC stars. This is the value that can be compared with observational data.

stars, namely the large excesses of Na that are often observed in GC stars, to trace these lost stars in the field. Figure 7 shows the run of [Na/Fe] among field stars, comparing it to the extremes of the distributions for GC stars. To this purpose, we collected data for field stars from three different sources: Gratton et al. (2003a); Venn et al. (2004), and Fulbright et al. (2007). Besides the abundance ratios, they indicated the population of each star on the basis of the kinematics. Gratton et al. divided stars into "accretion" and "dissipation", while Venn et al. used the more common separation between halo and disk. The correspondence accretion/halo and dissipation/disk is largely true for the stars in common. Finally, all stars from Fulbright et al. are bulge ones. In Fig. 7 we plot field stars -taken only once if they are present in more than one source- between metallicity −2.5 (to fit the lower limit of the GC metallicity range) and −1 (to avoid thin disk stars). In the upper panel we also plot $[Na/Fe]_{min}$ for our GCs, i.e. the original, first generation value that sits in the middle of the field stars distribution. In the lower panel we plot instead $[Na/Fe]_{max}$ for our GCs, i.e. the second generation value, well above the bulk of field stars.

Examining this plot, we find that, while most of the field stars roughly have [Na/Fe]$\lesssim$ 0, there are a few objects with rather large excess of Na, comparable to what is observed in second-generation stars of GCs. In the sample of 144 field stars with [Fe/H] < −1, there are six stars with [Na/Fe] > 0.3; for comparison, 50% (735 over 1483) of the stars in our survey of GC stars have these large Na excesses[8]. However, only two of these field stars are likely to be second-generation stars evaporated from GCs: HD74000 and HIP37335 (=G112-36). These two stars are also moderately depleted in Li (Hosford et al. 2009; Pilachowski et al. 1993), as expected for second generation stars in GCs (see Pasquini et al. 2005). The remaining four Na-rich stars are extremely metal-poor stars residing in binary systems, and the Na excess may be attributed to mass transfer. Two of them (CS22898027 and CS22947187) are C-rich stars. G246-38 is extremely Li-poor (Boesgaard et al. 2005). Finally, also HD178443 is a giant in a binary system. While the statistics are poor, we may conclude that some 1.4% of the field metal-poor stars are likely Na-rich stars evaporated from GCs. Since these are half of the GC stars, we may conclude that stars evaporated from GCs make up 2.8% of the metal-poor component of the Milky Way. We may compare this value with the current fraction of stars in GCs, which is 1.2% using the Juric et al. (2008) in situ star counts and 5% using the Morrison (1993) ones. We neglect the impact of selective loss of low-mass stars; this is not too bad an approximation because spectroscopic data are only available for stars with typically the current TO mass. We conclude that the GCs should have made up some 4% of the original mass of metal-poor stars, if Juric et al. star counts are used, and as much as 7.8% adopting the Morrison ones. These values may still be underestimates. In fact, if the cooling flow scenario is correct, second-generation stars were originally a very kinematically cold population, which means that they evaporated from the GCs only after dynamical relaxation led to energy equipartition, ∼1 Gyr after the GC formation, i.e., much later than the formation phase. Then, there should be many more primordial stars of GCs now in the field, lost during the early phases. As discussed above, these values should be increased by an order of magnitude.

The conclusion is that precursors of GCs probably had a baryonic mass ∼20 times higher than the current mass (if both the efficiency of star formation and the huge star loss factors are taken into account). If they also contained dark matter, they were likely to be two orders of magnitudes greater than they currently are, with total masses up to a few 10^8 $M_{\odot}$, which is the size of dSph's (see also Bekki et al. 2007).

We propose that the fraction of the primordial population lost by GCs is a major building block of the halo, although we do not exclude other minor contributors. This is supported by many other arguments, including their total mass, the metallicity distribution, and the location within the Milky Way, all of which are discussed in a separate paper (Gratton et al. 2010). GCs might have played a similar role in the formation of the metal-poor component of the thick disk ([Fe/H]< −1), while the specific frequency is much lower (by an order of magnitude) for the metal-rich component ([Fe/H]> −1), and they are obviously absent from the thin disk.

The formation phase of GCs may be very important for understanding star formation in the early phases of the Milky Way (and probably of other galaxies). Any information on the composition of the primordial population would help to shed light

[8] We only considered those GCs with [Fe/H] < −1. This ratio does not change significantly if we compute the fraction of Na-rich stars in each cluster and then average this value. In this way we underestimate the fraction of second generation stars, but we use this value here for consistency with the field stars.

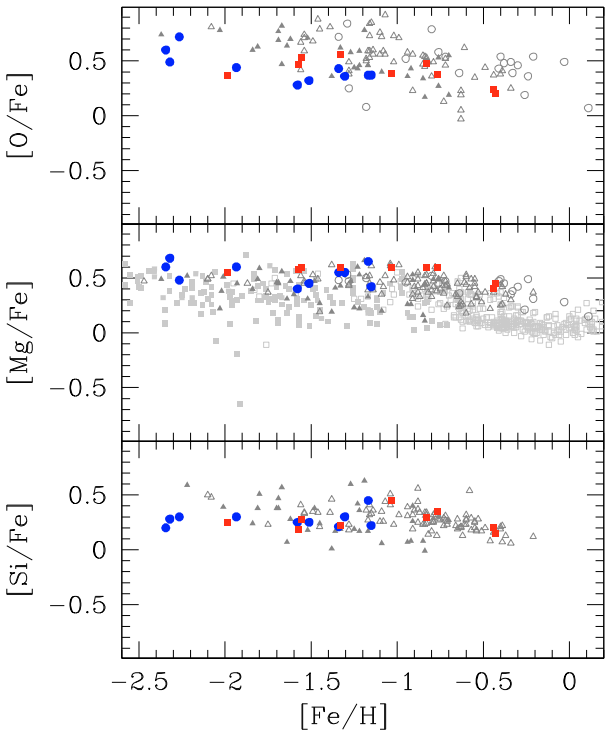

Fig. 8. $[O/Fe]_{max}$, $[Mg/Fe]_{max}$, $[Si/Fe]_{min}$ for our programme clusters (large filled red squares for disk/bulge clusters and blue circles for inner halo clusters, here and in the following figures) as a function of the metallicity [Fe/H], superimposed to field stars from literature (grey symbols).

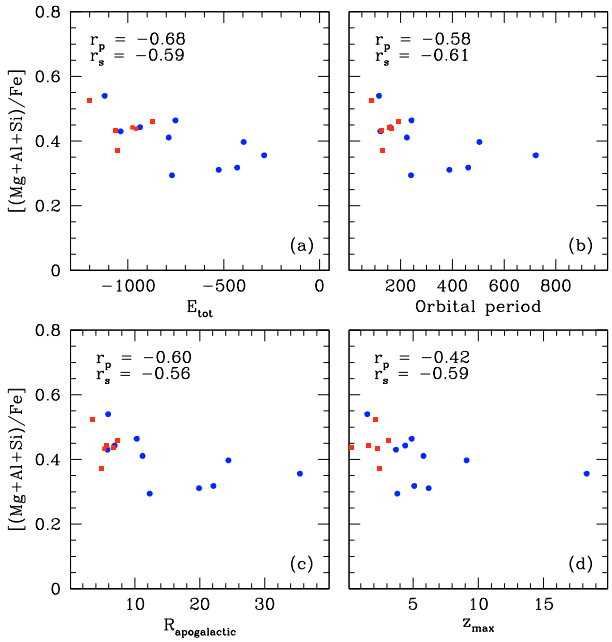

Fig. 9. Relation of the ratio [(Mg+Al+Si)/Fe] as a function of several orbital parameters: **a)** total energy of the orbit; **b)** orbital period; **c)** apogalatic distance, and **d)** maximum distance above the Galactic plane. Also indicated are the Spearman and Pearson correlation coefficients.

on the formation mechanism of GCs. We now examine what evidence can be obtained from our data.

4.2. The chemical evidence: the primordial abundance ratios and the scenario for GC formation

4.2.1. α-elements

As demonstrated by several authors (Gratton et al. 1996, 2000, 2003a, 2003b; Fuhrmann 1998, 2004), the [α/Fe] ratio is a good population discriminator. Nissen & Schuster (1997) found that halo subdwarfs have an [α/Fe] ratio on average lower and with more scatter than what is typical of the thick disk population at the same metallicity, a result later confirmed by several other investigations (see e.g. Gratton et al. 2003b).

While several of the α-elements are involved in the nuclear cycles related to high-temperature H-burning, there are many possible indicators of the primordial [α/Fe] ratio that we can obtain from our data. A short list includes the maximum O and Mg abundances ($[O/Fe]_{max}$ and $[Mg/Fe]_{max}$), the minimum Si abundance ($[Si/Fe]_{min}$), the total Mg+Al+Si content [(Mg+Al+Si)/Fe] (see Sect. 3.4 and footnote there), and the average of $[Mg/Fe]_{max}$, $[Si/Fe]_{min}$, and the typical α-element Ca. All these indicators give concordant results. In the following, we mainly use the total [(Mg+Al+Si)/Fe] content.

In Fig. 8 we plotted the run of the original abundance ratio of various α-elements with [Fe/H]: $[O/Fe]_{max}$, $[Mg/Fe]_{max}$, and $[Si/Fe]_{min}$. In the same figure, we also plotted the distribution of field stars from Fulbright (2000), Gratton et al. (2003a), Reddy et al. (2006), Venn et al. (2004) and Fulbright et al. (2003, 2006). GCs lie close to the location of the field stars, especially considering possible offsets among different analyses.

We do not have any a priori idea of what we should expect for the exact form of most of the relations between the new parameters we are introducing and global cluster parameters, so we adopt the simpler, linear relation. These relations are evaluated using the Pearson coefficient for linear regressions and the Spearman coefficient of rank correlation, which can be used to characterise the strength and direction of a relationship of two given random variables (e.g. Press et al. 1992).

Tight relations are obtained between the overabundance of α-elements (represented e.g., by Mg+Al+Si) and orbital parameters (confirming earlier findings by Lee & Carney 2002). In Fig. 9 we show the relations of the ratio [(Mg+Al+Si)/Fe] with total energy of the orbit, orbital period, apogalactic distance, and the maximum distance above the Galactic plane. The correlation coefficients, represented by the Spearman and Pearson coefficients (r_s and r_p), are high, and they would increase further by excluding NGC 5904 (M 5), the cluster affected by the largest uncertainties in the orbit.

Similar trends are seen when plotting the overabundance of Ca or the average between Ca and Ti I. It seems that clusters populating large-sized, more eccentric orbits with large apogalacticon distances (i.e., mostly the inner halo GCs, in our classification) also have a proclivity toward a lower abundance of elements produced in α-capture processes. We consider these results as an indication that the initial position affected the chemical enrichment of GCs

Is there a risk of a bias introducing spurious trends among orbital and chemical parameters? The correlation existing in our sample between absolute magnitude M_V and distance (Sect. 3.3) is not a source of concern. We find that the total Mg+Al+Si sum is anticorrelated (with moderate significance, between 90 and 95%) with M_V: the [(Mg+Al+Si)/Fe] ratio is lower in more massive clusters. However, we found that there is a slight trend for orbital parameters to be *correlated* with the cluster mass (luminosity) for our distance-limited sample. Although scarcely

significant from a statistical point of view, this trend is also present in the control sample of GCs with $D_{sun} < 12.9$ kpc and known orbital parameters. Thus, when taken together, these opposite trends should combine in such a way as to erase any dependence of the total Mg+Al+Si sum on orbital parameters, whereas we find good and significant relations. As a result, these trends are probably significant and should be considered when discussing scenarios for cluster formation.

We conclude that disk and halo GCs share the same [α/Fe] ratio of thick disk and halo stars respectively. As observed in the field, halo GCs have a smaller excess of α-elements on average, and a scatter larger than observed for the (thick) disk populations. From the [α/Fe] ratios collected in the Appendix, we find that below a metallicity of [Fe/H]= −1, the average values are +0.42 ± 0.01 dex (rms = 0.05 dex from 15 GCs) for disk/bulge clusters and +0.36 ± 0.02 dex (rms = 0.07 dex from 14 GCs) for inner halo ones.

The explanation that we propose here is not the classical one requiring the contribution of SNe Ia to raise the iron content, hence lower the [α/Fe] ratio. We propose the possibility that the contribution of core-collapse SNe to metal enrichment is weighted towards higher-mass SNe for the precursors of lower-mass clusters. The most kinematically energetic products (rich in particular in α-elements) might have been lost in more massive GCs, due to a powerful wind. Evidence of such a wind is found around very massive and young star clusters, such as the one observed in NGC 6946 (Sanchez Gil et al. 2009). In the Milky Way, these massive GCs are mainly found in the inner halo. This explanation is substantiated by the comparison of M 5 and M 4, providing a solution to the conundrum described in Sect. 3.3.

4.2.2. Aluminium

In Paper VIII we presented the run of $[Al/Fe]_{min}$ with [Fe/H] in GCs. $[Al/Fe]_{min}$ is expected to represent the Al abundance of the primordial population. We underlined there the large scatter observed in this diagram, which exceeds the observational uncertainties by far. We also noticed that there is a group of clusters, mainly belonging to the inner halo, characterised by very low values of $[Al/Fe]_{min}$. Similar results were previously obtained for individual clusters (see e.g. Melendez & Cohen 2009), but our extensive survey shows that this is a widespread property of GCs.

However, Fe is not the best reference element for Al, because it has a very different nucleosynthesis. Cleaner insight can be obtained considering Mg as reference. Mg and Al may both be produced by massive stars exploding as core collapse SNe. While Mg is an α-rich element whose production is primary, Al requires the existence of free neutrons for its synthesis, and therefore its production is sensitive to the initial metallicity (Arnett & Truran 1969; Truran & Arnett 1971; Woosley & Weaver 1995). The exact dependence of the ratio of Al to Mg as a function of overall metallicity has never been defined satisfactorily by theory, but it should show some sort of secondary behaviour with respect to Mg.

Figure 10 shows the run of $[Al_{min}/Mg_{max}]$ (that is, the ratio for the primordial population) with $[Mg_{max}/H]$ for our programme cluster. We also plot the run of [Al/Mg] with [Mg/H] for metal-poor field stars in the Milky Way (Fulbright et al. 2007; Reddy et al. 2003; Gehren et al. 2006; Jonsell et al. 2005; Fulbright 2000), as well as for stars in dSph galaxies (Koch et al. 2008; Geisler et al. 2004; Shetrone et al. 2001, 2003; Sbordone et al. 2004). As shown by Gehren et al. (2006), the local subdwarfs have markedly different [Al/Mg], depending on their

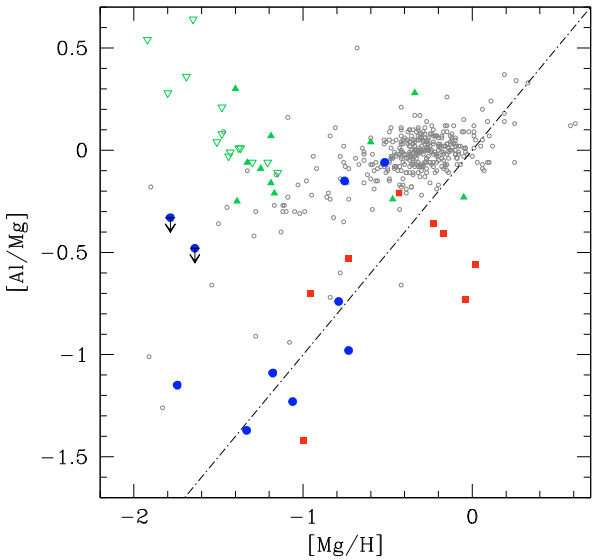

Fig. 10. Run of the [Al/Mg] ratio as a function of the [Mg/H] ratio in field stars (grey-tone open circles), GCs in our sample (red and blue filled circles and squares, respectively) and stars in dSphs (green triangles, the open ones are upper limits in Al, see text for references). The [Al/Mg] ratio in our sample refers to primordial abundances, namely $[Al/Fe]_{min}$ and $[Mg/Fe]_{max}$. The dot-dashed line indicate the line of secondary production [Al/Mg]=[Mg/H].

kinematics: halo subdwarfs have much lower [Al/Mg] than thick disk ones, so much so that Gehren et al. propose using this ratio as a population diagnostics. The locus occupied by primordial populations in most GCs is clearly distinct from the one for the thick disk subdwarfs and close to the one defined by halo subdwarfs. Several clusters, including the most massive ones, have very low primordial Al abundances and lie close to the line of secondary production: [Al/Mg] = [Mg/H]. The exception consists in a few small clusters (NGC 288, NGC 6121, NGC 6171, NGC 6838), which have large primordial Al abundances. A multivariate analysis, using $[Mg_{max}/H]$ and M_V as independent variables, and $[Al_{min}/Mg_{max}]$ as dependent one, yields

$$[Al_{min}/Mg_{max}] = (-0.01 \pm 0.24) + (0.66 \pm 0.14)[Mg_{max}/H] + (0.13 \pm 0.06)(M_V + 7.5), \quad (1)$$

with a highly significant linear correlation coefficient of $r = 0.80$ (16 clusters, 13 degrees of freedom). This behaviour is different from what is observed in dSphs, which are typically characterised by rather large Al abundances.

4.2.3. A scenario for the formation of GCs

How can we explain this behaviour? First, the *primary-like* run of Mg and Al observed in disk subdwarfs requires that most of the Al in these stars be produced in a different site from massive stars (where the production is secondary). Second, we observed very high Al_{max} abundances within second generation stars in GCs (Paper VIII and Table 2) even exceeding the values observed in disk subdwarfs and similar to those observed in dSph's stars. This suggests an obvious astrophysical site where these large amounts of Al can be produced: the same stars responsible for the Mg-Al anticorrelation (either fast-rotating massive stars – FRMS – or intermediate-mass AGB stars). In this case, the very low Al abundances, characteristic of the primordial population of massive GCs, may be explained *if the rise in metal content in the environment where these stars formed was so fast that no*

star with intermediate metallicity could form. On the other hand, pre-enrichment should have had to be more gradual for low-mass clusters, with different generations making little difference in the Mg content, and an efficient re-processing of Mg into Al in the next generation. A similar conclusion was drawn for the case of M 71 (NGC 6838) by Melendez & Cohen (2009). However, we find that this is a general feature of GCs, even of clusters reputed to be younger than the disk ones. This is unlikely to be a coincidence, but is instead more probably related to the typical sequence of events that led to cluster formation.

This consideration suggests a (still qualitative) sketch for the formation of typical massive GCs, which is a more elaborated and updated version of what was proposed more than thirty years ago by Searle & Zinn (1978) and later elaborated on by many other authors (see e.g. Böker 2008, and references therein).

1. Consider a cosmological fragment/satellite of 10^6–10^9 $M_\odot$ i.e. the same range of masses of dSph's, but which is near the Milky Way ($R_{GC} \sim 10$ kpc) at a very early epoch (<2 Gyr from the Big Bang). In a cold dark matter (CDM) scenario, we expect many such satellites to have existed (see e.g. Bromm & Clarke 2002; De Lucia & Helmi 2008). At this very early epoch, this satellite is still made of dark matter and gas (10^5–10^8 $M_\odot$), with negligible/small stellar contribution and metal pre-enrichment, depending on its age, i.e., on the time allowed for an isolated evolution before the phases described in the following.
2. Likely due to its motion, which brings the cluster in proximity of the denser central region of the Milky Way, this fragment has a strong interaction, possibly with the same early disk of the Milky Way or with another substructure (Bekki 2004). This strong interaction triggers an early star formation (Whitmore & Schweizer 1995). On a short timescale (a few million years) 10^4–10^5 $M_\odot$ of gas are transformed into stars. The most massive of these stars explode as SNe after $\sim 10^7$ yr. Hereinafter, we call this population *precursor*, because while needed to form the GC itself, it is unlikely that we will find any representative of this population within the present GC (see below).
3. The precursor core-collapse SNe have two relevant effects: i) they enrich the remaining part of the fragment/satellite of metals, raising its metallicity to the value currently observed in the GC[9]; and ii) efficiently trigger star formation in the remaining part of the cloud, before the intermediate mass stars can efficiently contribute to nucleosynthesis. This second episode (or phase, since it is not clear that there should not be a continuum in star formation) forms a few 10^5–10^6 $M_\odot$ of stars in a large association. These associations have mass and size (~100 pc) comparable to the knots commonly observed in luminous and ultra-luminous infrared galaxies (see e.g. Rodriguez Zaurin et al. 2007).
4. The strong wind from massive stars and core collapse SNe of this huge association disperses the remaining primordial gas on a timescale of $\sim 10^7$ yr (see the case of the super star cluster in NGC 6946, Sanchez Gil et al. 2009).
5. While the large association is expanding, the low-velocity winds from FRMS or, perhaps more likely[10], from the more massive intermediate-mass stars feed a cooling flow, which forms a kinematically cool population at the centre of the association (D'Ercole et al. 2008). Possible examples of objects in this phase are Sandage-96 in NGC 2403 (Vinko et al. 2009) or the super star cluster in NGC 6946 (Hodge 1967; Larsen & Richtler 1999; Larsen et al. 2006). A fraction of the primordial population stars (but very few precursors if any, since they are much rarer and possibly were at some distance from the newly forming cluster) remains trapped into the very compact central cluster formed by this second generation stars. This is the GC that may survive over a Hubble time, depending on its long-scale dynamical evolution and that we observe at present.
6. Core-collapse SNe from this second generation sweep the remaining gas within the cluster, terminating this last episode of star formation. This occurs earlier in more massive clusters: these clusters will then be enriched by stars over a restricted range of mass (only the most massive among the potential polluters), leading to very large He abundances. As a result, there should be correlations between He enrichment, cluster mass, and fraction of primordial stars. However, this may occur naturally only in a cooling flow scenario, where second generation star formation is well separated from the evolution of individual stars. In the original FRMS scenario of Decressin et al. (2008), second generation stars form within the individual equatorial disks around the stars, as a consequence of the large mass loss rate and fast rotation. Within this scenario, it is difficult (although not strictly impossible) to link properties of individual stars to global cluster properties.
7. At some point during these processes or just after, the DM halo is stripped anyway from the GC and merges with the general DM halo (see e.g. Saitoh et al. 2006; Maschenko & Sills 2005). It is not unlikely that the loss of the DM halo stems from the same interaction which causes the formation of the GC. The cluster has now acquired the typical dynamical characteristics that we observe at present, and hereinafter has essentially a passive evolution (see e.g. Ashman & Zepf 1992).

Small and/or metal-rich clusters (mainly residing in the disk) differ in many respects. Forming within a disk (not necessarily the disk of the main galaxy), they present a considerable pre-enrichment of metals. In the smaller clusters, the precursor population (if it exists) does not enrich the next generation significantly, which will share the chemical composition of the field. Moreover, as we recall in Sect. 3.3, the typical luminosity of disk GCs is lower than for halo GCs. A large fraction of disk stars form in small clusters and association, which are easily disrupted because of infant mortality and dynamical evolution. This might be closely related to the low specific frequency of clusters in spirals (Harris & Racine 1979; Harris 1988). In addition, dynamical interaction with the disk or the presence of other nearby star-forming regions might delay or reduce the efficiency of cooling flows in forming second-generation stars. Observations of many clusters with multiple turn-off's in the Magellanic Clouds (Mackey et al. 2008; Milone et al. 2009) might indicate that this effect is not so important; see, however, Bastian & De Mink (2009) for a different interpretation

[9] This enrichment should be very uniform, suggesting a super-wind from the precursor association (Mac Low & McCray 1988). There might also be a selection effect against the most massive and energetic SNe, possibly reducing the typical [α/Fe] ratio of the next generation stars.

[10] Given the very fast evolutionary lifetimes of FRMS, it is possible that the SN explosions from this component would hamper the formation of an efficient cooling flow.

Table 4. Pearson's correlation coefficients and level of significance for relations in *P*, *I*, and *E* stars.

Par	IQR	*P*	*I*	*E*
IQR[O/Na]		+0.25, <90%	−0.49, 95–98%	+0.65, >99%
P	+0.25, <90%		−0.91, >99%	+0.56, >99%
I	−0.49, 95–98%	−0.91, >99%		−0.85, >99%
E	+0.65, >99%	+0.56, 98−99%	−0.85, >99%	
[(Mg+Al+Si)/Fe]	−0.56, >99%	−0.59, 99%	+0.69, >99%	−0.73, >99%
[Ca/Fe]	+0.03, <90%	−0.43, 90–95%	+0.52, 98%	−0.51, 95–98%
$[O/Fe]_{min}$	−0.79, >99%	−0.37, <90%	+0.62, >99%	−0.78, >99%
$[O/Fe]_{max}$	−0.23, <90%	−0.12, <90%	+0.40, 90–95%	−0.67, >99%
$[Na/Fe]_{min}$	−0.03, <90%	+0.13, <90%	−0.20, <90%	+0.27, <90%
$[Na/Fe]_{max}$	−0.26, <90%	−0.26, <90%	+0.21, <90%	−0.10, <90%
$[Al/Fe]_{min}$	−0.46, 95%	−0.26, <90%	+0.36, <90%	−0.35, <90%
$[Al/Fe]_{max}$	+0.10, <90%	+0.49, 95−98%	−0.38, <90%	+0.10, <90%
$[Mg/Fe]_{max}$	−0.42, 95%	−0.55, 98−99%	+0.74, >99%	−0.80, >99%
$[Mg/Fe]_{min}$	−0.48, 95−98%	−0.61, >99%	+0.67, >99%	−0.56, 98−99%
$[Si/Fe]_{max}$	−0.47, 95-98%	−0.21, <90%	+0.32, <90%	−0.38, 90%
$[Si/Fe]_{min}$	−0.44, 95%	−0.32, <90%	+0.40, 90–95%	−0.40, 90–95%
[Fe/H]	+0.18, <90%	+0.01, <90%	−0.28, <90%	+0.58, 98−99%
M_V	−0.46, 95−98%	−0.39, 95%	+0.55, 98−99%	−0.61, >99%
age	−0.33, <90%	−0.40, 95%	+0.59, >99%	−0.71, >99%
$T_{\rm eff}^{\rm max}$(HB)	+0.69, >99%	+0.45, 95%	−0.47, 95–98%	+0.36, <90%

Notes. The number of degrees of freedom is generally 17, except for the cases involving [(Mg+Al+Si)/Fe], $[Al/Fe]_{min}$, and $[Al/Fe]_{max}$, where it is 16.

of these observations. Finally, disk GCs all formed very early in the Galactic history (Fall & Rees ; Zinn 1988). After these very early phases, conditions within the Milky Way disk were never again suitable for forming very massive GCs, most likely because the low pressure characteristic of quiet disks (Ashman & Zepf 2001).

As noticed by Zinn (1985), within this scheme the different chemical histories of disk and halo GCs may easily explain the most obvious characteristics of GCs, systematically observed in virtually all GC systems, such as: i) the bimodal colour and metallicity distribution, because blue clusters are essentially self-enriched, while red clusters form from pre-enriched material in the early phases of dissipational collapses (note, however, that there should be a few blue and metal-poor disk clusters); ii) the absence of discernible metallicity trends with $R_{\rm GC}$ for halo GCs (see Searle & Zinn 1978); and iii) the presence of relatively young GCs in the halo (Zinn 1985).

This scenario also unifies the view of GCs and dSphs. In fact, according to this scheme, both GCs and dSphs start as DM-dominated cosmological structures with masses in the range 10^6–10^9 $M_\odot$. The main difference is their location with respect to the Galaxy. GCs formed from DM haloes closer to the centre of the Galaxy or to other structures (even NGC 2419, the farthest known GC). They had only a limited significant, independent chemical evolution prior to their interaction with the Galaxy, which occurred quite early, when the structures were still gas-rich. The age-metallicity relation for halo GCs (see Fig. 5) suggests that pre-cluster clouds that had more time to evolve actually produced part of their metals during this pre-cluster phase. When they interacted with other structures or with the main Galaxy body itself, their independent evolution was interrupted by the sequence of phases we described above (see Melendez & Cohen 2009, for a similar view).

On the other hand, dSphs formed much farther, at typical distances of several hundred kpc. They could have a long independent evolution before interaction (if any) with the Milky Way. Their evolution is determined essentially by their initial mass, so that they obey mass-luminosity and mass-metallicity relations. If any interaction with the Milky Way has occurred (as is the case for Sagittarius), this happened once the dSph had become gas poor, and this did not lead to any further GC formation (although more massive dSphs could include a few already formed GCs).

As noticed by the referee, the scenario we considered implies that significant GC formation may still occur in gas-rich environments insofar as the high pressure needed is available, e.g. owing to galaxy-to-galaxy interaction. This is possibly the case of the Antennae (Whitmore & Schweizer 1995) or even of the Magellanic Clouds, where there is evidence of formation of six young clusters in the Magellanic Bridge (Irwin et al. 1985).

5. The second phase of cluster self-enrichment

In our scenario, the early phases of the evolution of the structures that will ultimately form GCs are linked to the composition of the primordial population, and the late phases determine the cluster self-enrichment processes. We expect that such processes are linked to some global characteristic of GCs. In Papers VII and VIII we showed that very important rôles are played by mass and metallicity of the cluster. In this Section, we revisit this issue, considering many other parameters; a more global approach will be applied in next Section.

5.1. The chemistry of second generation stars

The chemical properties of second-generation stars in GCs were discussed quite extensively in Papers VII and VIII. They may be described by the fraction of the intermediate I and of the extreme E components, and by the extreme values associated to the polluted stars using a dilution model, namely $[O/Fe]_{min}$, $[Na/Fe]_{max}$, $[Mg/Fe]_{min}$, $[Al/Fe]_{max}$. In Paper VIII we demonstrated that the ratio $[Si/Fe]_{max}$ is an additional marker of second-generation stars, because of the leakage of the Mg-Al cycle which produces ^{28}Si at temperatures in excess of about 65 million K (Carretta et al. 2009b; Arnould et al. 1999; Yong et al. 2005).

In Table 4 we list Pearson's correlation coefficients, the number of degrees of freedom, and the statistical significance level

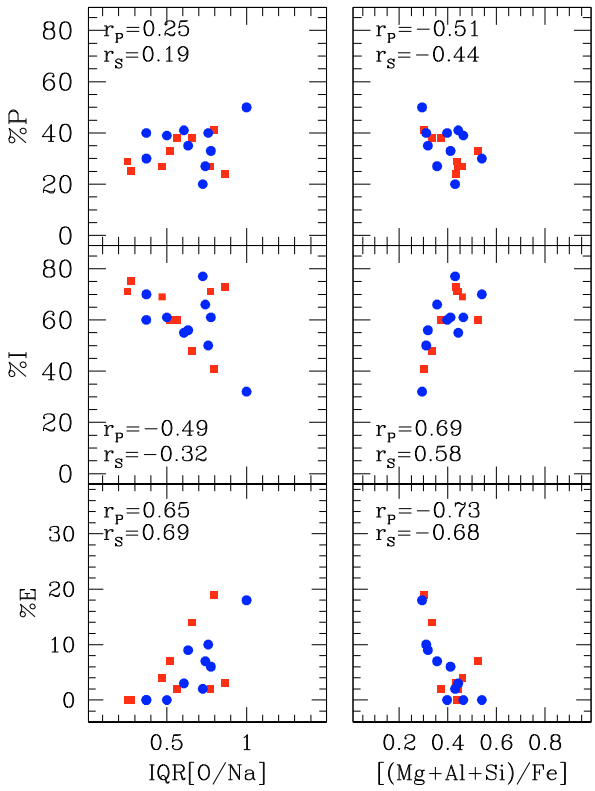

Fig. 11. *Left*: fraction of stars in the primordial P (*upper panel*), intermediate I (*middle panel*) and extreme E (*lower panel*, with a different scale on the *y*-axis) components of GCs as a function of the IQR[O/Na]. *Right*: the same, as a function of [(Mg+Al+Si)/Fe]. The Pearson and the Spearman rank correlation coefficients are shown in the box, here and in the next figures.

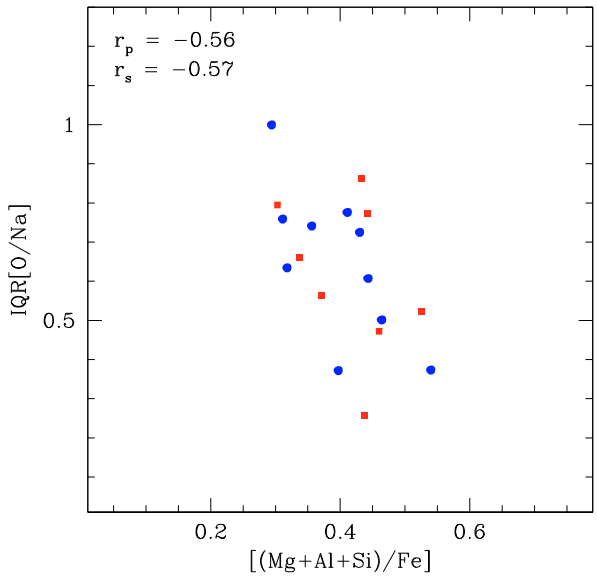

Fig. 12. Extension of the Na-O anticorrelation, measured by the IQR[O/Na], as a function of the total sum of Mg+Al+Si atoms for our sample of clusters.

of the correlations involving the extremes of the abundance distributions and the fraction of P, I, and E stars. In addition, we also considered the interquartile of the Na-O distribution IQR[O/Na][11]. We find several correlations with a high level of statistical significance (better than 99%), as can be seen from the table. The most interesting correlations are shown in Figs. 11 to 16.

From Table 4 and the lefthand panels in Fig. 11, we see that there is a tight correlation between the E fraction and the extension of the Na-O anticorrelation, IQR[O/Na]. This does not come as a surprise, since IQR[O/Na] is driven by the stars with extreme chemical modifications. The I fraction, which is the dominant group in all GCs, is anticorrelated with IQR[O/Na], while the primordial P component is not related to the extension of the Na-O anticorrelation.

The run of the P, I, and E fractions as a function of the total Mg+Al+Si sum is illustrated in the lefthand panels of Fig. 11. The fraction of stars in the P population is higher when this total sum is lower. Even tighter relations exist for the I and E components. The sign of these relations is opposite to those with IQR[O/Na]. The combination of the left and right panels in Fig. 11 results in the statistically significant anticorrelation between IQR[O/Na] and total Mg+Al+Si sum shown in Fig. 12: clusters where the Na-O anticorrelation is more extended have a lower value of the total Mg+Al+Si sum. This result is confirmed by the relations existing between the P, I, and E fractions and [Ca/Fe] (right panels in Fig. 13). However, we also notice that these findings are strongly influenced by the two bulge clusters NGC 6388 and NGC 6441.

The E population is the only one showing a significant correlation with [Fe/H]. However, this is not surprising, because we found (Carretta et al. 2009a) that O_{min}, whose value is related to the presence of the E component, is well represented by a linear combination of M_V and [Fe/H]. We interpreted this result as a proof that the mass of the average polluters varies regularly as a function both of cluster mass and metal abundance.

In Fig. 14 (right panels), the fractions of first and second generation stars are shown as a function of the relative GC ages. These relations are statistically significant, because the P and E components are anticorrelated and the I fraction correlated with age. This result might be an artefact owing to the relations with M_V (left panels of the same figure). As seen in Sect. 3, the more massive clusters in our sample are those in the inner halo, where the younger clusters reside. However, we cannot exclude other factors; for instance, the presence of a population with enhanced He might alter the derivation of ages, as discussed in detail in Gratton et al. (2010).

In summary, we find the following:

(i) A P component of first generation stars is present in each GC. Its incidence does not depend on the cluster metallicity, being approximatively constant (at a level of about one third of the cluster stars, Paper VII) in each GC. This component does not affect the extension of the Na-O anticorrelation, but it is less conspicuous in GCs with higher abundances of α-elements.

[11] We verified that the corresponding quantity for the Mg-Al anticorrelation IQR[Mg/Al] shows a general correlation with IQR[O/Na], with some scatter. However, IQR[Mg/Al] could only be estimated for the comparatively few stars observed with UVES. Furthermore, we could not compute this index for four GCs of our sample, because three only had 5–7 UVES spectra per cluster (NGC 6171, NGC 6388, and NGC 6441) and one without Al determination (NGC 6397). Thus, IQR[Mg/Al] has large uncertainties and will not be used in the rest of this paper. On the other hand, the IQR[O/Na] for NGC 6397, based on only 16 stars, is quite indiscernible from the others (based on more stars) in all relations shown in the following. This also supports the robustness of this indicator for the GC in our sample with the smallest number of sampled stars.

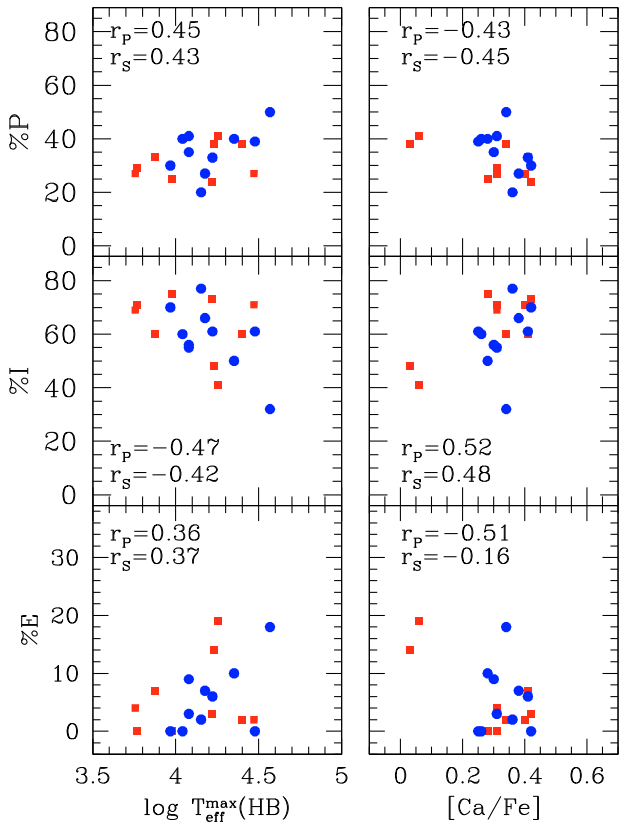

Fig. 13. *Left*: fraction of stars of the P, I, and E components (*upper, middle, and lower panels*, respectively) as a function of $\log T_{\rm eff}^{\rm max}$(HB). *Right*: the same, as a function of the mean [Ca/Fe] ratio.

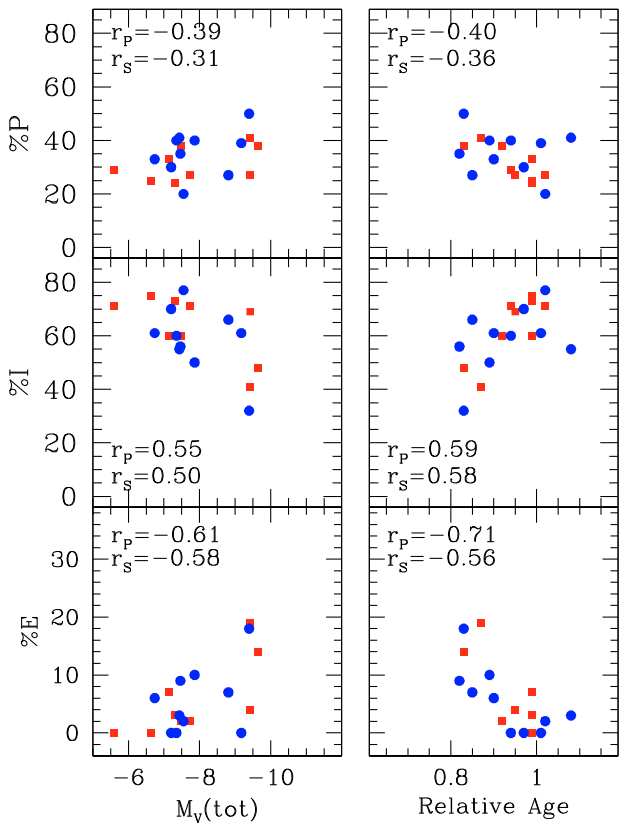

Fig. 14. *Left panels*: the fraction of stars in the P, I, and E components of second-generation stars as a function of the total absolute magnitude (hence, mass) of clusters. *Right*: the same, as a function of relative age.

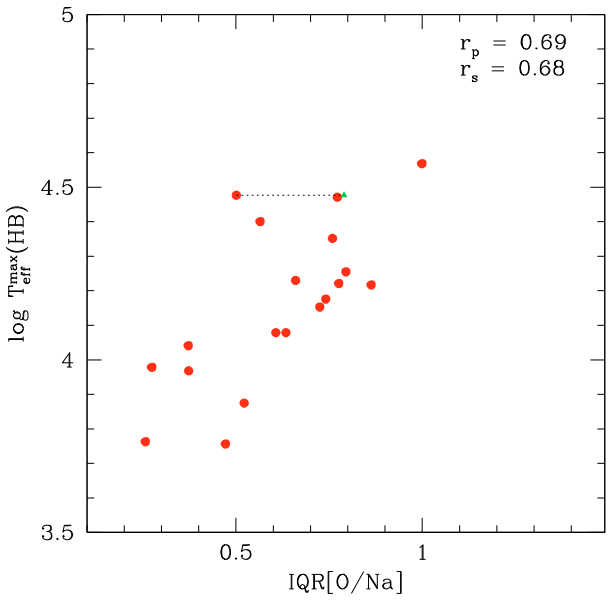

Fig. 15. Interquartile range of the [O/Na] ratio as a function of the maximum temperature reached on the HB (taken from Recio-Blanco et al. (2006) or derived here). The line connects the value for M 15 based on our data and the one derived from the literature (open green triangle, see text).

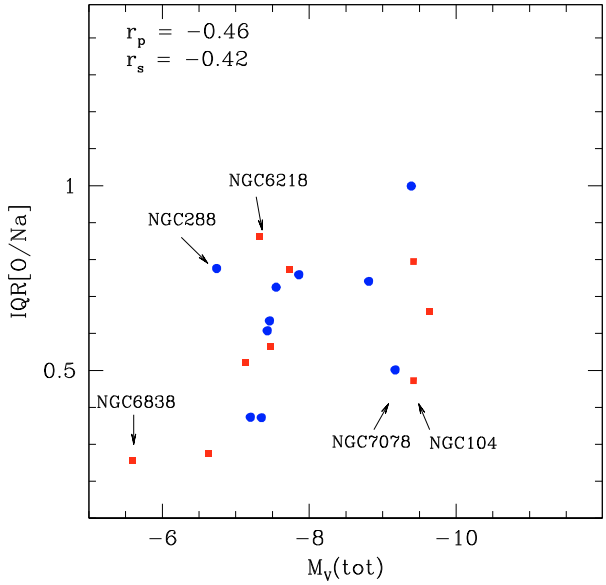

Fig. 16. The extension of the Na-O anticorrelation (measured using IQR[O/Na]) as a function of the clusters' absolute magnitude M_V from Harris (1996). The Pearson correlation coefficient is given and five GCs discussed in the text are indicated.

(ii) The bulk of second generation stars is composed of stars with moderate alterations in the light elements Na, O, Mg, Al participating to proton-capture reactions in H-burning at high temperature (see Paper VII). This I component is lower in GCs with longer Na-O anticorrelations, and this fraction is higher in GCs with larger α-element ratio.

(iii) The E component, with extreme changes in light element abundances with respect to first generation stars, is not present in all clusters (Paper VII). It is anticorrelated to the complementary I component and is the key component driving the extension of the Na-O anticorrelation, showing a very tight and significant correlation with IQR[O/Na]. The

E component decreases with increasing overabundance of α-elements.

In the following, we analyse the relations between the chemistry of different subpopulations and global cluster parameters.

5.2. Extension of the Na-O anticorrelation and (blue) HB

We demonstrated in Carretta et al. (2007d) that there is a tight correlation between IQR[O/Na] (derived from part of our sample or from the literature) and the maximum temperature of HB stars, $\log T_{\rm eff}^{\rm max}$(HB) (Recio-Blanco et al. 2006). To verify that this relation also holds for the more extended sample of clusters considered here, we complemented the values of $\log T_{\rm eff}^{\rm max}$(HB) obtained by Recio-Blanco et al. with new ones. We employed good quality CMDs (Bellazzini et al. 2001 for NGC 288; Marino et al. 2008 for NGC 6121; Rosenberg et al. 1999 for NGC 6254; Momany et al. 2003 for NGC 6752; Vargas Alvarez & Sandquist 2007 for NGC 6809) with the same HB models (Cassisi et al. 1999) as used by those authors. Furthermore, we replaced the values of IQRs of Carretta et al. (2007d) that were derived from the limited samples of stars with UVES spectra available at the time, with new ones obtained from the full sample of stars with Na and O determinations from GIRAFFE and UVES in all the 19 GCs in our sample (Table 2). We fully confirm our previous findings, as seen in Fig. 15[12].

The position of M 15 (NGC 7078) in Fig. 15 is somewhat uncertain. The value from literature lies very well on the sequence defined by all other clusters, while the value we derive is more offset from the main trend. Since M 15 is among the most metal-poor GCs and our GIRAFFE resolution is worse than the one in Sneden et al. (1997), it is possible that we missed some very O-poor or Na-poor stars. However, the O abundance of two most O-poor stars in Sneden et al. is flagged as uncertain. With these caveats in mind, we adopt here the value of the IQR[O/Na] for M 15 derived in our analysis for homogeneity. The correlation is at any rate very tight: the Spearman test returns coefficients r_S of 0.69 (with our value for M 15), 0.82 (with M 15 from literature), or 0.81 (without M 15). The probability of getting such a tight relation by chance is negligible, because the (one-tailed) t-test returns values of 2×10^{-4}, 1×10^{-6}, or 4×10^{-6} in the three cases, respectively.

We confirm that this is a real, very strong relation: the first conclusion we can draw is that the same mechanism drives or affects the extent of the pollution on the RGB and the morphology of the bluest end of the HB. However, this can be only considered *a* second parameter, because the global distribution of stars on the HB [as indicated e.g., by the HB ratio HBR=(B-R)/(B+R+V) – see Harris 1996 and web updates] is *not* correlated with IQR[O/Na], i.e. with the extension of the Na-O anticorrelation, as already discussed by Carretta (2006) and Carretta et al. (2007d). The relation between the distribution of stars along the HB and the Na-O anticorrelation is discussed further in a separate paper (Gratton et al. 2010).

Finally, the relations of the three individual stellar components P, I, E with $\log T_{\rm eff}^{\rm max}$(HB), shown in the right panels of Fig. 13, simply reflect the correlations and anticorrelations of the latter with IQR[O/Na].

[12] These results would not change had we used older parameters measuring the length of the HB, such as $L_{\rm tail}$ or BT from Fusi Pecci et al. (1993).

5.3. Extension of the Na-O anticorrelation and total cluster mass

Possibly a major result of our analysis is the good correlation we found between the IQR[O/Na] and the present-day total mass of the GCs (using the absolute magnitude M_V as a proxy for the mass), see Table 4 and Fig. 16. A high mass seems to be a prerequisite for an extended anticorrelation. This is not unexpected, because Recio-Blanco et al. (2006) have already found a good correlation between total mass and highest temperature on the HB, and in the previous section we found that the latter is strictly related to the extent of the Na-O anticorrelation.

The correlation found in Recio-Blanco et al. is also a good test of the reliability of our sample against a possible bias related to selection criteria. We do not have values for IQR[O/Na] for all clusters in the Harris catalogue; however, our distance-limited sample of 19 GCs shows a correlation between M_V and $\log T_{\rm eff}^{\rm max}$(HB), with a Pearson correlation coefficient $r_p = -0.47$, 17 degrees of freedom, significant at better than 95% level of confidence. The same correlation is present in all clusters in the Harris catalogue with available $\log T_{\rm eff}^{\rm max}$(HB) ($r_p = -0.43$, 54 GCs) and for clusters in the control sample restricted to distances less than 12.9 kpc from the Sun ($r_p = -0.52$, 42 GCs), both significant to more than 99%.

Thus this correlation does not come from selection bias. Moreover, since we included GCs with all morphologies of HB in our sample, it is not biased against HB type or $\log T_{\rm eff}^{\rm max}$(HB). It follows that the correlation we found between IQR[O/Na] and M_V is real.

The explanation of this correlation is quite complex. On one hand, it is clear that only massive enough clusters can have a second generation. However, i) (almost) all GCs are massive enough (while open clusters are probably not, see Fig. 3); and ii) IQR[O/Na] does not depend on the fraction of second generation stars (that is on $I+E$, or $P = 1-(I+E)$). Rather, IQR[O/Na] is correlated with E, and anticorrelated with I (see left panels of Fig. 11). This indicates that what is related to M_V is the extreme of the anti-correlation, not its median value. This has already been found in Papers VII and VIII, where we showed that $O_{\rm min}$ and $Al_{\rm max}$ are strongly correlated with a combination of M_V and [Fe/H]. In these papers we connected this to the typical mass of the polluters: the higher this mass, the higher the H-burning temperature, the lower $O_{\rm min}$ and the higher $Al_{\rm max}$.

As a result, available data indicate that the typical polluter's mass is related to M_V (i.e., total cluster mass). To explain this relation, either the maximum or the minimum mass (or both) defining the range of polluters is changing. This might be understood quite easily in the case of AGB polluters. The maximum mass may be reduced if the cooling flow is delayed by the effect of adjacent regions where massive stars are still present, as expected e.g. from formation of clusters in a spiral arm. The minimum mass may be higher in more massive clusters: the higher the cluster mass, the faster the critical mass needed for second generation star formation is reached, before the earliest second-generation SNe explode, halting star formation. In the case of massive stars polluters, the arguments are more complex but similar. Only stars formed by the ejecta of the most massive stars may contribute if the cluster mass is very high, perhaps due to devastating effect of super-winds blowing in very massive clusters.

However, the scatter we observe in Fig. 16 suggests that high mass alone is not a sufficient condition. Clusters lying off the global relation, at the left edge, namely NGC 288, NGC 6218, (M 12), and NGC 6838 (M 71) might be reconciled with the

bulk of other clusters if we assume that they lost a higher-than-average fraction of their original mass. We already gave in Sect. 4.1 arguments suggesting that a noticeable fraction of the original mass of GCs is lost after the formation phase. We searched the literature for observational evidence. De Marchi et al. (2006) argue for severe tidal stripping in NGC 6218, and they estimate that the present mass of this cluster might even be only one fifth of the original one. The flat mass function of NGC 6218 is also consistent with a large fraction of stars lost by evaporation or tidal stripping. A tidal tail is also suspected to be associated to NGC 288 (Leon et al. 2000), although other studies (Kiss et al. 2007) find no extended extra-tidal structures. The most intriguing evidence of high mass loss in these later phases is maybe the one for M 71. It comes from a totally independent line of thought. With its total absolute magnitude of $M_V = -5.6$ (Harris 1996), this cluster is the least massive object in Fig. 16. Elsner et al. (2008) published a study based on *Chandra* X-ray observations of M 71, where they find that there is an excess of sources for the present cluster mass, with respect to the relation defined by 47 Tuc, M 4, and NGC 6397. Another way to state the problem is that to bring M 71 on the relation given by the other clusters one must assume that 50 to 70% of its original mass was lost in the past. Elsner et al. use scaled values of the mass M_h inside the half-mass radii and a relation by Kong et al. (2006) linking M_h to the cluster absolute visual magnitude. Using the same relation, but assuming that the scaled mass of M 71 is 1 instead of 0.3, we get a value of $M_V = -7.2$ which would shift this cluster on the relation between IQR[O/Na] and M_V.

On the other hand, even if accounting for less massive clusters were possible, some problems are also left at the high-mass end. A high mass is not always matched by a very extended Na-O anticorrelation. NGC 104 (47 Tuc) is a notable example, because this cluster simply does not show very O-poor stars and presents a short/normal Na-O anticorrelation even if it is a very massive object. Some other factors must be involved. We reconsider the case of 47 Tuc in Gratton et al. (2010).

6. The next level of the game and conclusions

In the previous sections, as well as in Papers VII and VIII, we have seen the key rôle of the main parameters affecting the formation and early evolution of GCs, namely: (i) the mass; (ii) the metallicity; and (iii) the Galactic population/region to whom they belong (inner/outer halo vs disk). These main parameters summarise the history of a GC well, in the context of the evolution of the Galaxy itself. The correlations with chemical properties suggest that both the initial conditions at cluster's birth and the subsequent evolution while orbiting the Galaxy determine the resulting ratio of first and second generation stars and several other properties.

The next step is to systematically explore all the possible relations between the chemical signatures (in particular of second-generation stars) of GCs and global cluster parameters, to see whether they are independent relations or may be explained with a combination of these three main parameters. We can divide the parameters into five broad groups: i) structural parameters (including HBR, concentration c, ellipticity, r_h, r_t, and $\log T_{\rm eff}^{\rm max}$(HB)); ii) orbital parameters and/or parameters depending on the location in the Galaxy (R_{GC}, $|Z|$, E_{tot}, age, M_V, [Fe/H][13]); iii) primordial abundances ([(Mg+Al+Si)/Fe] and average [α/Fe]) and first generation ones (Mg_{max}, Si_{min}, Al_{min}, Na_{min}, O_{max}, plus fraction of P stars); iv) chemical parameters of second-generation stars (Mg_{min}, Si_{max}, Al_{max}, Na_{max}, O_{min}, and fractions of I and E stars); and v) parameters linking first and second generation stars (slope of the [Al/Fe] vs [Na/Fe] ratios and IQR[O/Na])[14].

The GC family is a complex one, with properties depending on many often interconnected parameters (see e.g., Djorgovski & Meylan 1994). While finding dependencies of a particular cluster property on others may be a viable approach, a more comprehensive and detailed analysis should take all clusters' parameters into account using a multivariate approach, so we applied the principal component analysis (PCA) on our set. This method has been used many times to understand the properties of the GC system (e.g., Fusi Pecci et al. 1993; Djorgovski & Meylan 1994; Recio-Blanco et al. 2006), but this is the first time that it is also extended to the properties of the different stellar generations in GCs. The method finds the correlation matrix of the whole parameter set and defines the dimensionality of the data set, i.e., the minimum number of dimensions required to fully explain the data.

Unfortunately, a rigourous study using the PCA is hampered by i) the limited sizes of the sample, only 19 GCs, since this is the only set for which detailed and homogeneous abundances of first and second generation stars are available at present; and ii) the fact that not all parameters are available for all (neither for the same) clusters. We first tried it on the maximum sample for which all the 34 above-mentioned parameters are available. This means 15 GCs, where NGC 6388 and NGC 6441 were excluded because they do not have orbital information, NGC 6397, because we did not measure Al, and NGC 288 because it lacks a measure of ellipticity in Harris (1996). However, excluding four clusters could result in loss of significance in some cases. For instance, α-elements show a good correlation with M_V in our complete sample, but not in the reduced one, possibly because two very massive clusters are excluded. We repeated the analysis using the whole GC sample, excluding those parameters that were absent for at least one of the GCs, which was possible for 21 parameters.

We give in Table 5 (only available on-line) the complete list of the correlation coefficients among the 21 parameters. We show in Fig. 17 four examples, one taken from the first computation (E_{tot}) and three from the second one (M_V, [Fe/H], and age). The correlation coefficients are for linear relations. Table 6 gives information on the dimensionality (the number of eigenvalues larger than 1, the limiting value usually assumed in this kind of analysis) and on the fractional and cumulative contributions of the components. This table refers to both cases: 34 parameters for 15 GCs (first four columns) and 21 parameters for 19 GCs (last four columns). In the first case, the dimensionality is eight, the first three eigenvalues only account for 62% of the total variance, while eight components account for 93%. In the second case, the dimensionality is five (or six), the first three eigenvalues account for 66% of the total variance, while five (six) components account for 83 (87)%.

Besides monovariate relations, we tried a semiempirical approach to explore the dependencies of cluster parameters from the fundamental quantities. In particular, we wanted to test whether the key parameters mass, metallicity, age, and orbital elements (the last two representing the position in the Galaxy) are

[13] [Fe/H] was included in this group to take into account that inner halo GCs are on average more metal-poor than disk clusters.

[14] We used here all the possible indicators of chemistry in first and second generation stars because some are affected by saturation (e.g., Na_{min} and O_{max}) and others only show a small variation from the original value (e.g., Si).

Table 5. Correlation coefficients for 21 parameters of the 19 GCs.

	M_V 1	HBR 2	[Fe/H] 3	r_h 4	log $T_{\rm eff}^{\rm max}$ 5	Relage 6	IQR 7	%*P* 8	%*I* 9	%*E* 10	⟨SiCa⟩ 11	[α/Fe] 12	O_{min} 13	O_{max} 14	Mg_{min} 15	Mg_{max} 16	Na_{min} 17	Na_{max} 18	Si_{min} 19	Si_{max} 20	Z 21
1	–	0.304	–0.293	0.113	–0.433	0.387	–0.463	–0.393	0.551	–0.614	0.533	0.495	0.495	0.375	0.564	0.336	–0.350	0.074	0.349	0.178	0.071
2	0.304	–	–0.731	0.131	0.454	0.407	0.198	–0.204	0.329	–0.420	0.128	0.178	0.121	0.366	0.096	0.224	–0.657	–0.181	–0.244	–0.254	–0.229
3	–0.293	–0.731	–	–0.187	–0.195	–0.549	0.182	0.003	–0.277	0.585	–0.142	–0.252	–0.387	–0.658	0.045	–0.310	0.661	0.271	0.026	–0.034	0.070
4	0.113	0.131	–0.187	–	–0.157	0.005	0.138	–0.214	0.195	–0.131	0.439	0.376	–0.078	0.197	0.193	0.127	–0.146	–0.219	0.371	0.078	0.050
5	–0.433	0.454	–0.195	–0.157	–	–0.199	0.693	0.453	–0.468	0.361	–0.347	–0.333	–0.471	–0.056	–0.681	–0.272	–0.207	–0.389	–0.530	–0.334	–0.232
6	0.387	0.407	–0.549	0.005	–0.199	–	–0.332	–0.396	0.593	–0.710	0.464	0.592	0.707	0.603	0.425	0.752	–0.075	0.306	0.356	0.505	–0.167
7	–0.463	0.198	0.182	0.138	0.693	–0.332	–	0.248	–0.486	0.654	–0.188	–0.297	–0.788	–0.228	–0.475	–0.423	–0.030	–0.262	–0.438	–0.465	–0.207
8	–0.393	–0.204	0.003	–0.214	0.453	–0.396	0.248	–	–0.914	0.561	–0.484	–0.517	–0.372	–0.118	–0.615	–0.551	0.130	–0.263	–0.321	–0.206	–0.185
9	0.551	0.329	–0.277	0.195	–0.468	0.593	–0.486	–0.914	–	–0.848	0.573	0.661	0.621	0.398	0.671	0.740	–0.204	0.211	0.404	0.320	0.187
10	–0.614	–0.420	0.585	–0.131	0.361	–0.710	0.654	0.561	–0.848	–	–0.542	–0.680	0.621	–0.667	–0.559	–0.797	0.265	–0.097	–0.397	–0.378	–0.121
11	0.533	0.128	–0.142	0.439	–0.347	0.464	–0.188	–0.484	0.573	–0.542	–	0.957	0.218	0.368	0.503	0.630	0.012	–0.032	0.801	0.473	0.153
12	0.495	0.178	–0.252	0.376	–0.333	0.592	–0.297	–0.517	0.661	–0.680	0.957	–	0.345	0.419	0.485	0.805	0.054	0.053	0.784	0.547	0.060
13	0.495	0.121	–0.387	–0.078	–0.471	0.707	–0.788	–0.372	0.621	–0.779	0.218	0.345	–	0.486	0.462	0.598	–0.074	0.372	0.336	0.561	0.074
14	0.375	0.366	–0.658	0.197	–0.056	0.603	–0.228	–0.118	0.398	–0.667	0.368	0.419	0.486	–	0.219	0.477	–0.376	–0.352	0.089	0.157	0.292
15	0.564	0.096	0.045	0.193	–0.681	0.425	–0.475	–0.615	0.671	–0.559	0.503	0.485	0.462	0.219	–	0.486	0.036	0.350	0.386	0.224	0.156
16	0.336	0.224	–0.310	0.127	–0.272	0.752	–0.423	–0.551	0.740	–0.797	0.630	0.805	0.598	0.477	0.486	–	0.108	0.277	0.476	0.599	–0.007
17	–0.350	–0.657	0.661	–0.146	–0.207	–0.075	–0.030	0.130	–0.204	0.265	0.012	0.054	–0.074	–0.379	0.036	0.108	–	0.539	0.310	0.308	–0.349
18	0.074	–0.181	0.271	–0.219	–0.389	0.306	–0.262	–0.263	0.211	–0.097	–0.032	0.053	0.372	–0.352	0.350	0.277	0.539	–	0.176	0.330	–0.536
19	0.349	–0.244	0.026	0.371	–0.530	0.356	–0.438	–0.321	0.404	–0.397	0.801	0.784	0.336	0.089	0.386	0.476	0.310	0.176	–	0.721	0.061
20	0.178	–0.254	–0.034	0.078	–0.334	0.505	–0.465	–0.206	0.320	–0.378	0.473	0.547	0.561	0.157	0.224	0.599	0.308	0.330	0.721	–	0.120
21	0.071	–0.229	0.070	0.050	–0.232	–0.167	–0.207	–0.185	0.187	–0.121	0.153	0.060	0.074	0.292	0.156	–0.007	–0.349	–0.536	0.061	0.120	–

actually those giving the most significant relations with structural and chemical parameters of GCs. We derived the correlations for parameters chosen in all the groups defined above as a function of all bi-variate combinations of M_V, [Fe/H], age, and $E_{\rm tot}$; then, we counted the frequency of the most significant correlations (larger than 99%) for each combination in each group. The results are given in Table 7 (on-line only) and summarised in Table 8. The best combinations are essentially two: M_V-age and [Fe/H]-age.

Obviously, this is only meaningful if the main parameters we are using are independent. From the monovariate correlations we see that M_V is not correlated with age. A significant correlation does instead exist between [Fe/H] and age. This is evident both in our sample (Fig. 17) and in the global one of Galactic GCs (Fig. 5), and it is stronger when individual subpopulations (inner halo vs disk/bulge) are considered. However, the age-metallicity relation is a physical one, intrinsic to the system of GCs, and not a spurious bias affecting our sample. We may safely conclude that most of the "phenotypes" of GCs can be explained rather well by the variations of three fundamental parameters: total mass, metallicity, and age, linked by the origin and the interaction of GCs in, and with, our Galaxy.

In summary, in this paper we combine the results of our extensive survey of abundances in RGB stars in 19 GCs (Carretta et al. 2009a,b,c) with previous knowledge of a GC, in order to discuss scenarios for their formation. The novelty of our approach is to fully take into account the fact that GCs cannot anymore be regarded as simple stellar populations. For the first time it is possible to include among the properties of GCs a quantitative estimate of the ratio and of the chemical composition of different stellar generations. Our main findings are:

(i) We first analyse the definition of GCs. The presence of the Na-O anticorrelation may be very well used to separate GCs from smaller (open) clusters. Second, we divide GCs according to their kinematics and location in the Galaxy in three populations: disk/bulge, inner halo, and outer halo. We find that the LF of bona fide GCs (that is, those which exhibit the Na-O anticorrelation) is fairly independent of their population. This suggests that it is imprinted by the formation mechanism, and only marginally affected by the following evolution.

(ii) We then use the evidence of different generations within GCs given by their chemistry, and consider separately the composition of the primordial population and of the second generation. A large fraction of the primordial population should have been lost by the proto-GCs. We propose that the fraction of primordial population stars lost by GCs make up the main component of halo field stars. Arguments in favour include the total number of stars, the metallicity, kinematic and density distribution, and the chemistry.

(iii) In addition, we argue that the extremely low Al abundances found for the primordial population of massive GCs is an indication of a very fast enrichment process before the formation of the primordial population. We then suggest a scenario for the formation of GCs including at least three main phases: a) the formation of a precursor population (likely due to the interaction with the early Galaxy or with other cosmological structures similar to those that led to the formation of dwarf spheroidals, but residing at smaller Galactocentric distances); b) which triggers a large episode of star formation (the primordial population); and c) then the formation of the current GC, mainly within a cooling flow formed by the slow winds of a fraction of this primordial population.

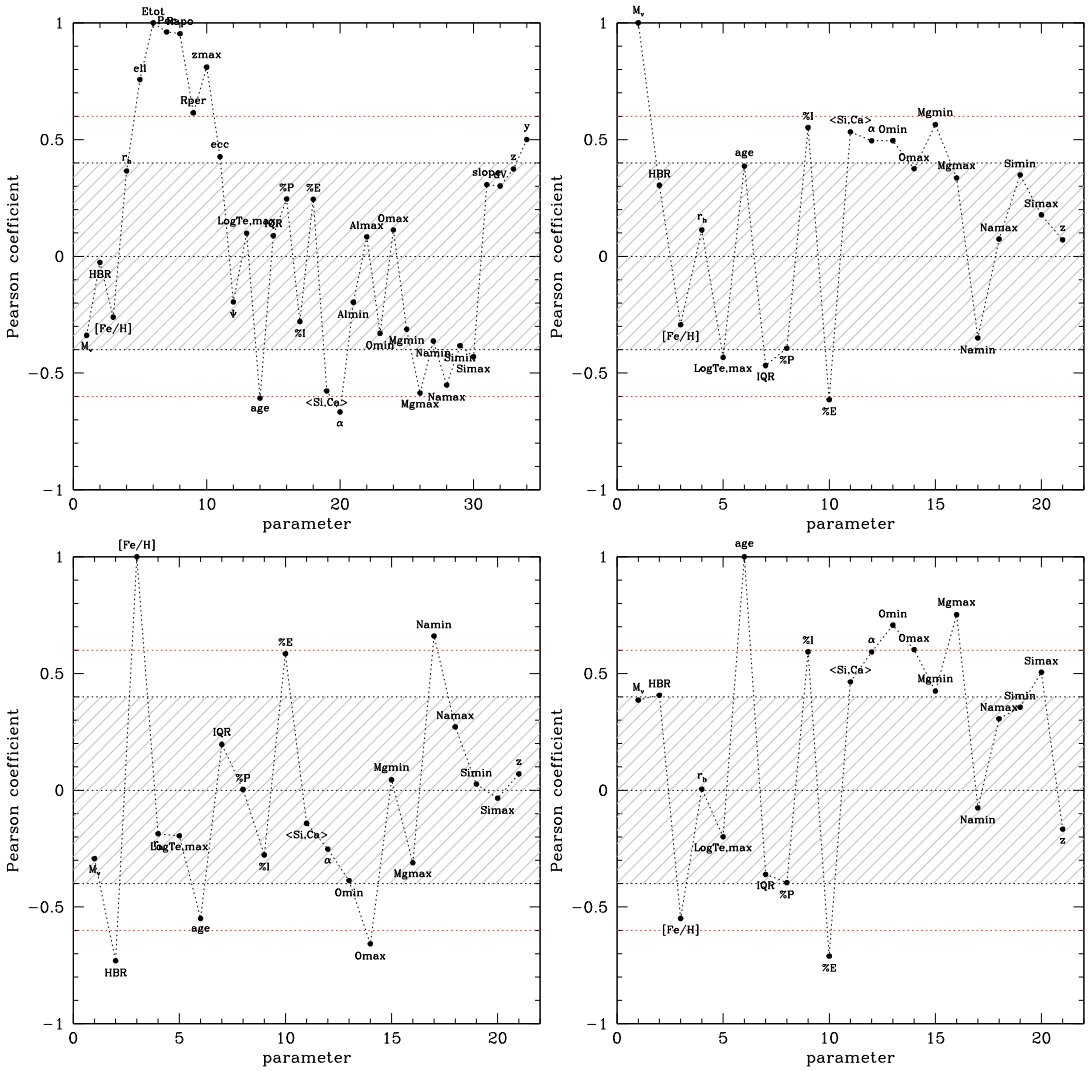

Fig. 17. Example of the linear monovariate correlations found for E_{tot} (*left upper panel*), M_V (*right upper panel*), [Fe/H] (*left lower panel*), and age (*right lower panel*). The first is for 15 GCs, the three other for 19 GCs. The grey zone indicates that there is no significant correlation, while the horizontal lines are drawn at (anti)-correlations larger than 0.4 and 0.6, which represent limits for a significance better than about 90% and 99% for our samples.

Some stars of the primordial population remains trapped in the newly forming cluster, producing the primordial component still observed in GCs. The precursor population is very effective in raising the metal content in massive and/or metal-poor (mainly halo) clusters, while its rôle is minor in small and/or metal rich (mainly disk) ones.

(iv) We then re-examine the second phase of metal-enrichment (from primordial to second generation): we consider monovariate, bivariate relations, and an explorative PCA. Our conclusion is that most of the "phenotypes" of GCs (and in particular their detailed chemical characteristics) may be ascribed to a few parameters, the most important being metallicity, mass, and age of the cluster. Location within the Galaxy (as described by the kinematics) also plays some rôle, while additional parameters are required to describe their dynamical status.

The proposed scenario for the origin of GCs offers a first framework to interpret the increasing information coming from spectroscopy and photometry of GCs, and implicitly suggests several tests that can be performed. Some are currently undertaken by our and other groups. Is it possible to reproduce the observed features of the HBs in term of the fundamental parameters

Table 6. Eigenvalues, fractional, and cumulative contributions for the two cases discussed in the text.

34 parameters, 15 GCs				21 parameters, 19 GCs			
i	e_i	V_i	C_i	i	e_i	V_i	C_i
1	11.35	33.39	33.39	1	8.25	39.30	39.30
2	5.19	15.28	48.67	2	3.61	17.18	56.48
3	4.52	13.28	61.95	3	2.11	10.05	66.53
4	2.99	8.79	70.73	4	1.86	8.83	75.36
5	2.40	7.06	77.79	5	1.56	7.51	82.87
6	2.06	6.17	83.96	6	0.96	4.57	87.44
7	1.76	5.17	89.13	7	0.69	3.20	90.74
8	1.16	3.42	92.55	8	0.61	2.91	93.65

mass, metallicity,and age (see e.g., Gratton et al. 2010)? Does the proposed scenario (precursor-present GC, which hosts multiple stellar generations) also valid outside the typical mass range of GCs? We are presently exploring both the very low-mass end, with the old open cluster NGC 6791, and the high-mass end, with M 54 (NGC 6715), and results will be published in the near future.

While corroborating evidence is coming from these studies, several issues are still dramatically open and/or poorly explored.

Table 7. Correlations, with number of clusters, degrees of liberty, Pearson coefficients (without sign), and significance in percent.

	M_V	[Fe/H]	age	$E_{\rm tot}$
	Structural parameters			
HBR	19 17 0.30 <90	19 17 0.73 >99	19 17 0.41 90–95	17 15 0.01 <90
c	19 17 0.35 <90	19 17 0.29 <90	19 17 0.31 <90	17 15 0.03 <90
ellipticity	18 16 0.36 <90	18 16 0.05 <90	18 16 0.44 90–95	16 14 0.61 98–99
$r_{\rm h}$	19 17 0.11 <90	19 17 0.19 <90	19 17 0.00 <90	17 15 0.33 <90
$r_{\rm t}$	19 17 0.33 <90	19 17 0.41 90–95	19 17 0.04 <90	17 15 0.59 98–99
log $T_{\rm eff}$	19 17 0.43 90–95	19 17 0.20 <90	19 17 0.20 <90	17 15 0.18 <90
	Orbital and positional parameters			
$R_{\rm GC}$	19 17 0.00 <90	19 17 0.30 <90	19 17 0.24 <90	17 15 0.59 98–99
$\|Z\|$	19 17 0.02 <90	19 17 0.40 90–95	19 17 0.07 <90	17 15 0.48 95.0
$E_{\rm tot}$	17 15 0.34 <90	17 15 0.20 <90	17 15 0.64 >99	
age	19 17 0.43 90–95	19 17 0.37 <90		17 15 0.78 >99
$M)V$		19 17 0.29 <90	19 17 0.39 90.0	17 15 0.34 <90
[Fe/H]	19 17 0.29 <90		19 17 0.55 98–99	17 15 0.20 <90
	Primordial abundances			
Mg+Al+Si	18 16 0.42 90–95	18 16 0.18 <90	18 16 0.77 >99	16 14 0.68 >99
α	19 17 0.49 95–98	19 17 0.25 <90	19 17 0.59 >99	17 15 0.64 >99
	First generation abundances			
$Mg_{\rm max}$	19 17 0.34 <90	19 17 0.31 <90	19 17 0.75 >99	17 15 0.61 99.0
$Si_{\rm min}$	19 17 0.35 <90	19 17 0.03 <90	19 17 0.36 <90	17 15 0.37 <90
$Al_{\rm min}$	18 16 0.19 <90	18 16 0.23 <90	18 16 0.23 <90	16 14 0.24 <90
$Na_{\rm min}$	19 17 0.35 <90	19 17 0.66 >99	19 17 0.08 <90	17 15 0.26 <90
$O_{\rm max}$	19 17 0.37 <90	19 17 0.66 >99	19 17 0.60 >99	17 15 0.00 <90
P	19 17 0.39 90.0	19 17 0.00 <90	19 17 0.40 90–95	17 15 0.33 <90
	Second generation abundances			
$Mg_{\rm min}$	19 17 0.56 98–99	19 17 0.04 <90	19 17 0.42 90–95	17 15 0.35 <90
$Si_{\rm max}$	19 17 0.18 <90	19 17 0.03 <90	19 17 0.51 95–98	17 15 0.46 90–95
$Al_{\rm max}$	18 16 0.26 <90	18 16 0.40 90.0	18 16 0.15 <90	16 14 0.13 <90
$O_{\rm min}$	19 17 0.50 95–98	19 17 0.39 90.0	19 17 0.71 >99	17 15 0.40 <90
$Na_{\rm max}$	19 17 0.07 <90	19 17 0.27 <90	19 17 0.31 <90	17 15 0.46 90–95
I	19 17 0.55 98–99	19 17 0.28 <90	19 17 0.59 >99	17 15 0.37 <90
E	19 17 0.61 >99	19 17 0.58 99.0	19 17 0.71 >99	17 15 0.34 <90
	Link first-second generation			
slope[Na/Al]	18 16 0.46 95.0	18 16 0.08 <90	18 16 0.35 <90	16 14 0.34 <90
IQR[O/Na]	19 17 0.46 95–98	19 17 0.18 <90	19 17 0.33 <90	17 15 0.18 <90

Table 8. Number of significant correlations with different class of parameters.

	Struct.	Orbit./ posit.	Primord. abund.	Chem. of FG	Chem. of SG	Total
M_V	0	0	0	0	1	1
[Fe/H]	1	0	0	2	0	3
age	0	1	2	2	3	8
$E_{\rm tot}$	0	1	2	0	0	3
$R_{\rm GC}$	0	1	0	0	0	1
M_V,[Fe/H]	1	0	0	2	2	5
M_V,age	1	1	2	2	4	10
M_V,$E_{\rm tot}$	3	1	2	1	0	7
M_V,$R_{\rm GC}$	0	1	0	0	3	4
[Fe/H],age	1	1	2	3	3	10
[Fe/H],$E_{\rm tot}$	2	1	2	1	0	6
[Fe/H],$R_{\rm GC}$	0	1	0	2	1	4
$E_{\rm tot}$,age	2	0	2	2	2	8
$R_{\rm GC}$,age	0	1	2	2	3	8
$R_{\rm GC}$,$E_{\rm tot}$	1	1	2	1	0	5

A full hydrodynamical treatment of the formation and early evolution of GCs is still missing, the relation between GCs and past and present dSphs needs to be well studied, the nature and the precise yields of candidate first generation polluters still have to be definitively assessed, the rôle of binaries has to be well understood; to mention only a few open problems. The road to a deeper understanding of the GCs has been opened in the past few years, but the way is still long.

Acknowledgements. We warmly thank Michele Bellazzini for useful discussions and a careful reading of the manuscript. The comments of the referee were very useful for producing a clearer manuscript. A.B. thanks the Observatoire de la Côte d'Azur for hospitality during the preparation of the paper. This research has made use of the SIMBAD database, operated at the CDS, Strasbourg, France, and of NASA's Astrophysics Data System. This work was partially funded by the Italian MIUR under PRIN 2003029437 and PRIN 20075TP5K9, and by INAF by the grant INAF 2005 "Experimenting nucleosynthesis in clean environments". S.L. acknowledges the support by the DFG cluster of excellence "Origin and Structure of the Universe".

References

Alonso, A., Arribas, S., & Martinez-Roger, C. 1999, A&AS, 140, 261
Alonso, A., Arribas, S., & Martinez-Roger, C. 2001, A&A, 376, 1039
Arnett, W. D., & Truran, J. W. 1969, ApJ, 157, 339
Arnould, M., Goriely, S., & Jorissen, A. 1999, A&A, 347, 572
Ashman, K. M., & Zepf, S. 1992, ApJ, 384, 50
Ashman, K. M., & Zepf, S. 2001, AJ, 122, 1888
Barbuy, B., Zoccali, M., Ortolani, S., et al. 2006, A&A, 449, 349
Barbuy, B., Zoccali, M., Ortolani, S., et al. 2007, AJ, 134, 1613
Bastian, N., & De Mink, S. 2009, MNRAS, 398, L11
Baumgardt, H., Kroupa, P., & Parmentier, G. 2008, MNRAS, 384, 1231
Bedin, L. R., Piotto, G., Anderson, J., et al. 2004, ApJ, 605, L125
Bekki, K. 2004, PASA, 21, 167
Bekki, K., & Chiba, M. 2002, ApJ, 566, 245
Bekki, K., & Chiba, M. 2007, ApJ, 665, 1164
Bekki, K., Campbell, S. W., Lattanzio, J. C., & Norris, J. E. 2007, MNRAS, 377, 335

Bekki, K., Yahagi, H., Nagashima, M., & Forbes, D. A. 2008, MNRAS, 387, 1131
Bellazzini, M., Fusi Pecci, F., Ferraro, F. R., et al. 2001, AJ, 122, 2569
Bellazzini, M., Perina, S., Galleti, S., et al. 2008a, MSAIt, 79, 663
Bellazzini, M., Ibata, R. A., Chapman, S. C., et al. 2008b, AJ, 136, 1147
Boesgaard, A. M., Stephes, A., & Deliyannis, C. P. 2005, ApJ, 633, 398
Böker, T. 2008, ApJ, 672, L111
Bragaglia, A., Carretta, E., & Gratton, R., et al. 2010, A&A, accepted
Bromm, V., & Clarke, C. 2002, ApJ, 566, L1
Brown, J. H., Burkert, A., & Truran, J. W. 1991, ApJ, 376, 115
Brown, J. H., Burkert, A., & Truran, J. W. 1995, ApJ, 440, 666
Brown, J. A., Wallerstein, G., & Zucker, D. 1997, AJ, 114, 180
Brown, J. A., Wallerstein, G., & Gonzalez, G. 1999, AJ, 118, 1245
Buonanno, R., Corsi, C. E., Zinn, R., et al. 1998, ApJ, 501, L33
Buonanno, R., Corsi, C. E., Castellani, V., et al. 1999, AJ, 118, 1671
Busso, G., Cassisi, S., Piotto, G., et al. 2007, A&A, 474, 105
Caputo, F., & Castellani, V. 1984, MNRAS, 207, 185
Carollo, D., Beers, T. C., Lee, Y. S., et al. 2008, Nature, 451, 216
Carretta, E. 2006, AJ, 131, 1766
Carretta, E., Gratton, R. G., Bragaglia, A., Bonifacio, P., & Pasquini, L. 2004, A&A, 416, 925
Carretta, E., Bragaglia, A., Gratton, R. G., et al. 2006, A&A, 450, 523 (Paper I)
Carretta, E., Bragaglia, A., Gratton, R. G., Lucatello, S., & Momany, Y. 2007a, A&A, 464, 927 (Paper II)
Carretta, E., Bragaglia, A., Gratton, R. G., et al. 2007b, A&A, 464, 939 (Paper IV)
Carretta, E., Bragaglia, A., Gratton, R. G., et al. 2007c, A&A, 464, 967 (Paper VI)
Carretta, E., Recio-Blanco, A., Gratton, R. G., Piotto, G., & Bragaglia, A. 2007d, ApJ, 671, L125
Carretta, E., Bragaglia, A., Gratton, R. G., et al. 2009a, A&A, 505, 117 (Paper VII)
Carretta, E., Bragaglia, A., Gratton, R. G., & Lucatello, S. 2009b, A&A, 505, 139 (Paper VIII)
Carretta, E., Bragaglia, A., Gratton, R. G., D'Orazi, V., & Lucatello, S. 2009c, A&A, 508, 695
Carretta, E., Bragaglia, A., Gratton, R. G., et al. 2010, ApJ, 714, L7
Casetti-Dinescu, D. I., Girard, T. M., Herrera, D., et al. 2007, AJ, 134, 195
Cassisi, S., Castellani, V., Defl'Innocenti, S., Salaris, M., & Weiss, A. 1999, A&AS,134, 103
Cavallo, R. M., Suntzeff, N. B., & Pilachowski, C. A. 2004, AJ, 127, 3411
Cayrel, R. 1986, A&A, 168, 81
Chabrier, G. 2003, PASP, 115, 763
Charbonnel, C., Brown, J. A., & Wallerstein, G. 1998, A&A, 332, 204
Chernoff, D. F., & Weinberg, M. D. 1990, ApJ, 351, 121
Clemens, D. P. 1985, ApJ, 295, 422
Cohen, J. G. 2004, AJ, 127, 1545
Cohen, J. G., & Melendez, J. 2005, AJ, 129, 1607
Cohen, J. G., Gratton, R. G., Behr, B. B., & Carretta, E. 1999, ApJ, 523, 739
D'Antona, F., & Caloi, V. 2008, MNRAS, 360, 693
D'Antona, F., & Ventura, P. 2007, MNRAS, 379, 1431
De Angeli, F., Piotto, G., Cassisi, S., et al. 2005, AJ, 130, 116
Decressin, T., Baumgardt, H., Kroupa, P., Meynet, G., & Charbonnel, C. 2008, ed. D. Soderblom, et al., IAU Symp. 258, [arXiv:0812.2912]
Decressin, T., Meynet, G., Charbonnel, C., Prantzos, N., & Ekstrom, S. 2007, A&A, 464, 1029
De Marchi, G., Pulone, L., & Paresce, F. 2006, A&A, 449, 161
Denisenkov, P. A., & Denisenkova, S. N. 1989, A. Tsir., 1538, 11
D'Ercole, A., Vesperini, E., D'Antona, F., McMillan, S. L. W., & Recchi, S. 2008, MNRAS, 391, 825
De Silva, G. M., Gibson, B. K., Lattanzio, J., & Asplund, M. 2009, A&A, 500, L25
D'Orazi, V., Lucatello, S., Gratton, R., et al. 2010, ApJ, 713, L1
Dinescu, D. I., Girard, T. M., & van Altena, W. F. 1999, AJ, 117, 1792
Djorgovski, S., & Meylan, G. 1994, AJ, 108, 1292
Elsner, R. F., Heinke, C. O., Cohn, H. N., et al. 2008, ApJ, 687, 1019
Fall, S. M., & Rees, M. J. 1985, ApJ, 298, 18
Fall, S. M., & Rees, M. J. 1988, in The Harlow-Shapley Symposium on Globular Cluster Systems in Galaxies (Dordrecht: Kluwer Academic Publishers), 323
Feltzing, S., Primas, F., & Johnson, R. A. 2009, A&A, 493, 913
Ferrario, L., Wickramasinghe, D., Liebert, J., & Williams, K. A. 2005, MNRAS, 361, 1131
Fraix-Burnet, D., Davoust, E., & Charbonnel, C. 2009, MNRAS, 398, 1766
Freeman, K. C. 1990, in Astrophysics – Recent progress and future possibilities, Copenhagen, Kongelige Danske Videnskabernes Selskab, 187
Fuhrmann, K. 1998, A&A, 338, 161
Fuhrmann, K. 2004, AN, 325, 3
Fulbright, J. P. 2000, AJ, 120, 1841
Fulbright, J. P., & Johnson, J. A. 2003, ApJ, 595, 1154
Fulbright, J. P., McWilliam, A., & Rich, R. M. 2006, ApJ, 636, 821
Fulbright, J. P., McWilliam, A., & Rich, R. M. 2007, ApJ, 661, 1152
Fusi Pecci, F., Ferraro, F. R., Bellazzini, M., et al. 1993, AJ, 105, 1145
Geisler, D., Bica, E., Dottori, H., et al. 1997, AJ, 114, 1920
Geisler, D., Harris, G. L. H., Reid, M., et al. 2004, A&AS, 204, 8009
Gratton, R. G. 2007, in From Stars to Galaxies: Building the Pieces to Build Up the Universe. ASP Conf. Ser., 374, 147
Gratton, R., Carretta, E., Matteucci, F., & Sneden, C. 1996, in Formation of the Galactic Halo...Inside and Out, ed. H. Morrison & A. Sarajedini, ASP Conf. Ser., 92, 307
Gratton, R., Carretta, E., Matteucci, F., & Sneden, C. 2000, A&A, 358, 671
Gratton, R. G., Bonifacio, P., Bragaglia, A., et al. 2001, A&A, 369, 87
Gratton, R. G., Carretta, E., Claudi, R., Lucatello, S., & Barbieri, M. 2003a, A&A, 404, 187
Gratton, R., Carretta, E., Desidera, S., et al. 2003b, A&A, 406, 131
Gratton, R. G., Sneden, C., & Carretta, E. 2004, ARA&A, 42, 385
Gratton, R. G., Lucatello, S., Bragaglia, A., et al. 2006, A&A, 455, 271 (Paper III)
Gratton, R. G., Lucatello, S., Bragaglia, A., et al. 2007, A&A, 464, 953 (Paper V)
Gratton, R. G., Carretta, E., Bragaglia, A., Lucatello, S., & D'Orazi, V. 2010, A&A, submitted
Harris, W. E. 1988, in The Harlow-Shapley Symposium on Globular Cluster Systems in Galaxies (Dordrecht: Kluwer Academic Publishers), 237
Harris, W. E. 1996, AJ, 112, 1487
Harris, W. E., & Racine, R. 1979, ARA&A, 17, 241
Hartwick, F. D. A. 2009, ApJ, 691, 1248
Hasegawa, K., Umemure, M., & Kitayama, T. 2009, MNRAS, 397, 1338
Hodge, P. W. 1967, PASP, 79, 29
Hosford, A., Ryan, S. G., Garcia Perez, A. E., Norris, J. E., & Olive, K. A. 2009, A&A, 493, 601
Irwin, M. J., Kunkel, W. E., & Demers, S. 1985, Nature, 318, 160
Ivans, I. 2009, BA&AS, 41, 205
Ivans, I., Kraft, R. P., Sneden, C., et al. 2001, AJ, 122, 1438
Ivans, I., Sneden, C., Wallerstein, G., et al. 2004, MSAIt, 75, 286
Jonsell, K., Edvardsson, B., Gustaffson, B., et al. 2005, A&A, 440, 321
Juric, M., Ivezic, Z., Brooks, A., et al. 2008, ApJ, 673, 864
Kiss, L. L., Szekely, P., Bedding, T. R., Bakos, G. A., & Lewis, G. F. 2007, ApJ, 659, L129
Koch, A., Mcwilliam, A., Grebel, E. K., Zucker, D. B., & Belokurov, V. 2008, ApJ, 688, L13
Kong, A. K. H., Bassa, C., Pooley, D., et al. 2006, ApJ, 647, 1065
Kraft, R. P. 1994, PASP, 106, 553
Kraft, R. P., Sneden, C., Smith, G. H., Shetrone, M. D., & Fulbright, J. 1998, AJ, 115, 1500
Kravtsov, A. V., & Gnedin, O. Y. 2005, ApJ, 623, 650
Kroupa, P., & Boily, C. M. 2002, MNRAS, 336, 1188
Langer, G. E., Hoffman, R., & Sneden, C. 1993, PASP, 105, 301
Larsen, S. S., & Richtler, T. 1999, A&A, 345, 59
Larsen, S. S., Origlia, L., Brodie, J. P., & Gallagher, J. S. 2006, MNRAS, 368, L10
Larson, R. B. 1987 in "Nearby normal galaxies", ed. S. Faber (NY: Springer), 26
Lata, S., Pandey, A. K., Sagar, R., & Mohan, V. 2002, A&A, 388, 158
Lee, J.-W. 2007, Rev. Mex. Astron. Astrofis., 28, 120
Lee, J.-W., & Carney, B. W. 2002, AJ, 124, 1511
Lee, J.-W., Carney, B. W., & Balachandran, S. 2004, AJ, 128, 2388
Lee, J.-W., Morales, M., & Carney, B. W. 2006, ApJ, 646, L119
Leon, S., Meylan, G., & Combes, F. 2000, A&A, 359, 907
Letarte, B., Hill, V., Jablonka, P., et al. 2006, A&A, 453, 547
Lind, K., Primas, F., Charbonnel, C., Grundahl, F., & Asplund, M. 2009, A&A, 503, 545
Lynden-Bell, D. 1967, MNRAS, 136, 101
Mackey, A. D., & Gilmore, G. F. 2003, MNRAS, 340, 175
Mackey, A. D., & van den Bergh, S. 2005, MNRAS, 360, 631
Mackey, A. D., Broby Nielsen, P., Ferguson, A. M. N., & Richardson, J. C. 2008, ApJ, 681, L17
Mac Low, M.-M., & Mc Cray, R. 1988, ApJ, 324, 776
Marcolini, A., Gibson, B. K., Karakas, A. I., & Sánchez-Blázquez, P. 2009, MNRAS, 395, 719
Marín-Franch, A., Aparicio, A., Piotto, G., et al. 2009, ApJ, 694, 1498
Marino, A. F., Milone, A. P., Piotto, G., et al. 2009, A&A, 505, 1099
Marino, A. F., Villanova, S., Piotto, G., et al. 2008, A&A, 490, 625
Martell, S. L., & Smith, G.H, 2009, PASP, 121, 577
McCarthy, J. K., & Nemec, J. M. 1997, ApJ, 482, 203
McWilliam, A., Geisler, D., & Rich, R. M. 1992, PASP, 104, 1193
Melendez, J., & Cohen, J. 2009, ApJ, 699, 2017
Miller, G. E., & Scalo, J. M. 1979, ApJS, 41, 513
Milone, A. P., Bedin, L. R., Piotto, G., & Anderson, J. 2009, A&A, 497, 755

Milone, A. P. et al 2010, ApJ, 709, 1183
Momany, Y., Cassisi, S., Piotto, G., et al. 2003, A&A, 407, 303
Morrison, H. L. 1993, AJ, 106, 578
Mottini, M., Wallerstein, G., & McWilliam, A. 2008, AJ, 136, 614
Murray, S. M., & Lin, D. N. C. 1992, ApJ, 400, 265
Nissen, P., & Schuster, W. J. 1997, A&A, 326, 751
Olsen, K. A. G., Hodge, P. W., Mateo, M., et al. 1998, MNRAS, 300, 665
Origlia, L., & Rich, R. M. 2004, AJ, 127, 3422
Origlia, L., Valenti, E., & Rich, R. M. 2005, MNRAS, 363, 897
Parmentier, G., & Gilmore, G. F. 2007, MNRAS, 363, 326
Parmentier, G., Goodwin, S. P., Kroupa, P., & Baumgardt, H. 2008, ApJ, 678, 347
Pasquini, L., Bonifacio, P., Molaro, P., et al. 2005, A&A, 441, 549
Peebles, P. J. E., & Dicke, R. H. 1968, ApJ, 254, 451
Pilachowski, C. A., Sneden, C., & Booth, J. 1993, ApJ, 407, 699
Piotto, G., Bedin, L. R., Anderson, J., et al. 2007, ApJ, 661, L53
Prantzos, N., & Charbonnel, C. 2006, A&A, 458, 135
Press, W. H., Teukolsky, S. A., Vetterling, W. T., & Flannery, B. P. 1992 (Cambridge: University Press), 2nd edn
Pritzl, B. J., Venn, K. A., & Irwin, M. 2005, AJ, 130, 2140
Ramirez, S., & Cohen, J. G. 2002, AJ, 123, 3277
Recio-Blanco, A., Aparicio, A., Piotto, G., De Angeli, F., & Djorgovski, S. G. 2006, A&A, 452, 875
Reddy, B. E., Lambert, D. L., & Allende Prieto, C. 2006, MNRAS, 367, 1329
Renzini, A. 2008, MNRAS, 391, 354
Rodríguez Zaurín, J., Holt, J., Tadhunter, C. N., & González Delgado, R. M. 2007, MNRAS, 375, 1133
Rosenberg, A., Saviane, I., Piotto, G., & Aparicio, A. 1999, AJ, 118, 2306
Russell, S. C. 1998, PASA, 15, 189
Saitoh, T. R., Koda, J., Okamoto, T., Wada, K., & Habe, A. 2006, ApJ, 640, 22
Salaris, M., Weiss, A., Ferguson, J. W., & Fusilier, D. J. 2006, ApJ, 465, 1121
Salpeter, E. E. 1955, ApJ, 121, 161
Sánchez Gil, M. C., Alfaro, E. J., & Pérez, E. 2009, ApJ, 702, 141
Saviane, I., Rizzi, L., Held, E. V., Bresolin, F., & Momany, Y. 2002, A&A, 390, 59
Sbordone, L., Bonifacio, P., Buonanno, R., et al. 2007, A&A, 465, 815
Sbordone, L., Bonifacio, P., Marconi, G., & Buonanno, R. 2004, MemSAIt, 65, 396
Searle, L., & Zinn, R. 1978, ApJ, 225, 357
Shetrone, M. D., & Keane, M. J. 2000, AJ, 119, 840
Shetrone, M. D., Côté, P., & Sargent, W. L. W. 2001, ApJ, 548, 592
Shetrone, M., Venn, K. A., Tolstoy, E., et al. 2003, AJ, 125, 684
Smith, G. H., & Martell, S. L. 2003, PASP, 115, 1211
Smith, G. H., Sneden, C., & Kraft, R. P. 2002, AJ, 123, 1502
Sneden, C. 2000, in The Galactic Halo: From Globular Cluster to Field Stars, ed. A. Noels, P. Magain, D. Caro, E. Jehin, G. Parmentier, & A. A. Thoul. Liege, Belgium: Institut d'Astrophysique et de Geophysique, 159
Sneden, C., Kraft, R. P., Shetrone, M. D., et al. 1997, AJ, 114, 1964
Sneden, C., Pilachowski, C. A., & Kraft, R. P. 2000, AJ, 120, 1351
Sneden, C., Kraft, R. P., Guhathakurta, P., Peterson, R. C., & Fulbright, J. P. 2004, AJ, 127, 2162
Suntzeff, N. B., & Kraft, R. P. 1996, AJ, 111, 1913
Suntzeff, N. B., Schommer, R. A., Olzsewski, E. W., & Walker, A. R. 1992, AJ, 104, 1743
Truran, J. W., & Arnett, W. D. 1971, Ap&SS, 11, 430
Tukey, J. W. 1977, in Box-and-Whisker Plots, Explanatory data analysis. Reading (MA: Addison-Wesley)
Vandenberg, D. A. 2000, ApJS, 129, 315
van den Bergh, S. 1981, A&AS, 46, 79
van den Bergh, S., & Mackey, A. D. 2004, MNRAS, 354, 713
Vargas Alvarez, C. A., & Sandquist, E. L. 2007, AJ, 134, 825
Venn, K., Irwin, M., Shetrone, M., et al. 2004, ApJ, 128, 1177
Ventura, P., D'Antona, F., Mazzitelli, I., & Gratton, R. 2001, ApJ, 550, L65
Vinko, J., Sarneczky, K., Balog, Z., et al. 2009, ApJ, 695, 619
Wheeler, J. C., Sneden, C., Truran, J. W. Jr. 1989, ARA&A, 27, 279
Whitmore, B. C., & Schweizer, F. 1995, AJ, 109, 960
Woosley, S. E., & Weaver, T. A. 1995, ApJS, 101, 181
Yong, D., & Grundahl, F. 2008, ApJ, 672, L20
Yong, D., Grundahl, F., Nissen, P. E., Jensen, H. R., & Lambert, D. L. 2005, A&A, 438, 875
Yong, D., Karakas, A. I., Lambert, D. L., Chieffi, A., & Limongi, M. 2008, ApJ, 689, 1031
Zinn, R. 1985, ApJ, 293, 424
Zinn, R. 1988, in The Harlow-Shapley Symposium on Globular Cluster Systems in Galaxies (Dordrecht: Kluwer Academic Publishers), 37

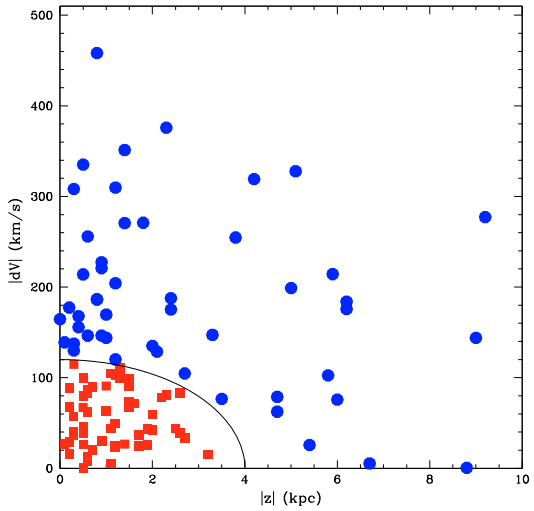

Fig. A.1. Classification of disk (red squares) and inner halo (blue dots) clusters. The curve is the discriminating line as obtained from our selection criteria.

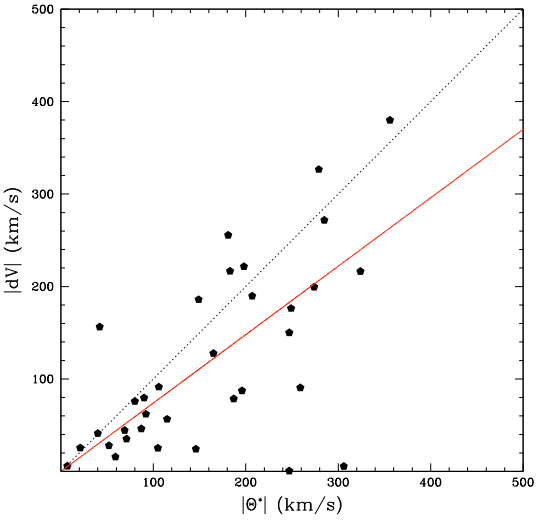

Fig. A.2. Absolute values of the difference dV between the observed radial velocity of GCs and the one expected from the Galactic rotation curve, as a function of the rotational velocity given by Dinescu et al. (1999) and Casetti-Dinescu et al. (2007). The dotted line indicates one-to-one correlation, while the red solid lines indicate the linear regression.

Appendix A: Classification of Galactic globular clusters

Since the work by Zinn (1985) a few progresses were done with respect to his criteria for the separation of the subpopulations of Galactic GCs. Many classification schemes rest on the appearance of the clusters' CMD and related parameters (namely metallicity, age and HBR index). However, one of the main aims of our project is to explain the HB morphology and its relations with chemical signatures of stellar generations in GC, so we cannot use the distribution of stars along the HB as a separation criterion. In Table A.1 we list the quantities used in Sect. 3.3 to separate disk/bulge clusters from the halo ones according to the combination of their location in the Galaxy and their kinematics.

As said in Sect. 3.3, outer halo clusters were simply classified as those currently located at more than 15 kpc from the centre of the Galaxy (see Carollo et al. 2008). Clusters with R_{GC} below 3.5 kpc were considered as bulge GCs, even though some of them might be halo clusters on very elongated orbits presently close to the pericentres. To separate the remaining clusters into inner halo and disk GCs, we computed the differences (dV, Col. 8 in Table A.1) between the observed radial velocity (corrected to the LSR) and the one expected from the Galactic rotation curve (see Clemens 1985). In the d$V - Z$ plane (where Z is the clusters' distance from the Galactic plane, in kpc, see Col. 10 of Table A.1), we defined an ellipse with equation

$$y = \left(\frac{|\mathrm{d}V|}{120}\right)^2 + \left(\frac{|z|}{4}\right)^2 .$$

Clusters with $y < 1$ were classified as disk GCs, while we considered as halo GCs the ones with $y > 1$, see Fig A.1. Of course, a better estimate of GC kinematic is possible when the whole orbit is available. Given the quite good correlation (see Fig. A.2) between dV and the rotational velocity (Col. 9 of Table A.1, where $\Theta^\star = \Theta - 220$) given by Dinescu et al. (1999) and Casetti-Dinescu et al. (2007), we replaced our dV values, when available, with the ones provided from those studies. Since we find that $|\mathrm{d}V| = (0.74 \pm 0.06)|\Theta^\star|$, the definition of y was in this case

$$y = \left(\frac{|\Theta^\star|}{162}\right)^2 + \left(\frac{|z|}{4}\right)^2 .$$

It should, however, be clear that dV is not at all a synonymous of (Θ-220), and the existing correlation has only a statistical meaning.

Column 11 in Table A.1 shows our classification for the population of the Galactic GCs in disk/bulge (D/B), inner halo (IH), outer halo (OH), and GCs of dSphs. For each cluster we report the integrated magnitude (M_V, Col. 2), the HB morphology parameter (HBR, Col. 6), and the Galactocentric distance (R_{GC}, Col. 7) as directly retrieved from the Harris catalogue. The metallicity values ([Fe/H], Col. 3) were instead replaced with the determinations by Carretta et al. (2009c). Additionally, we list in Col. 4 the [α/Fe] ratios (with corresponding references given in the table notes). Column 5 displays the age parameter; more in detail, we computed an average value between the two different estimates by Marin-Franch et al. (2009) and De Angeli et al. (2005), after applying a correction of 0.08 to the second ones for GCs with [Fe/H] ranging from –1.8 to –1.1 dex, as suggested by a cluster-to-cluster comparison. When neither of these estimates was available, we adopted the ones calculated by Vandenberg (2000), normalised to the Marin-Franch scale by assuming that 13.5 Gyr = 1.00. We then corrected the values so obtained for the difference between the metallicities considered in those papers and those listed in Carretta et al. (2009c), transformed into [M/H] using an average [α/Fe] of +0.4 (see Table 2). This correction was made using the sensitivity of age on metallicity given by Marin-Franch et al. (2009).

First, we decided to compare our new classification with the previous ones relying only on metallicity and HB morphology (see Sect. 3.3). As representative of this approach, we chose the work by Mackey & van den Bergh (2005). Briefly, they defined as disk component all the GCs with [Fe/H]>−0.8 dex; the so-called "old" halo and "young" halo clusters were then divided following Zinn (1993), namely by computing the offset in HB type -at a given metallicity- with respect to the fiducial line of the inner halo clusters[15]. GCs with an offset larger and

[15] Both Zinn (1993) and Mackey & van den Bergh (2005) labelled inner halo GCs the ones more metal-poor than [Fe/H]=−0.8 dex and located at Galactocentric distance less than 6 kpc.

Table A.1. Classification and main parameters adopted for GCs.

Name	M_V	[Fe/H]	[α/Fe]	⟨Age⟩	HBR	R_{GC} (kpc)	dV (km s^{-1})	$\Theta^\star$	Z (kpc)	Pop.
NGC 104	–9.42	–0.76	0.42(1)	0.95	–0.99	7.4	–15	59	–3.2	D/B
NGC 288	–6.74	–1.32	0.42(1)	0.90	0.99	12.0	1	247	–8.8	IH
NGC 362	–8.41	–1.30	0.30(2)	0.80	–0.87	8.9	–176	249	–6.2	IH
NGC 1261	–7.81	–1.27	–	0.79	–0.71	18.2	–	–	–12.9	OH
Pal 1	–2.47	–0.51	–	0.52	–1.00	17.0	–	–	3.6	OH
AM1	–4.71	–1.84	–	–	–0.93	123.2	–	–	–91.3	OH
Eridanus	–5.14	–1.44	–	0.71	–1.00	95.2	–	–	–59.6	OH
Pal 2	–8.01	–1.29	–	–	–	35.4	–	–	–4.3	dSph
NGC 1851	–8.33	–1.18	0.38(3)	0.81	–0.36	16.7	–	87	–6.9	OH
NGC 1904	–7.86	–1.58	0.31(1)	0.89	0.89	18.8	–	137	–6.3	OH
NGC 2298	–6.30	–1.96	0.50(4)	1.01	0.93	15.7	–	246	–3.0	OH
NGC 2419	–9.58	–2.20	0.20(5)	–	0.86	91.5	–	–	35.9	OH
Pyxis	–5.75	–1.33	–	–	–1.00	41.7	–	–	4.8	OH
NGC 2808	–9.39	–1.18	0.33(1)	0.83	–0.49	11.1	–26	146	–1.9	IH
E3	–2.77	–0.73	–	0.92	–	7.6	–	–	–1.4	D/B
Pal 3	–5.70	–1.67	–	0.83	–0.50	95.9	–	72	61.8	OH
NGC 3201	–7.46	–1.51	0.33(1)	0.82	0.08	8.9	–458	521	0.8	IH
Pal 4	–6.02	–1.46	–	0.76	–1.00	111.8	–	–	103.7	OH
NGC 4147	–6.16	–1.78	0.38(6)	0.96	0.55	21.3	–	174	18.8	dSph
NGC 4372	–7.77	–2.19	–	1.00	1.00	7.1	–91	106	–1.0	D/B
Rup 106	–6.35	–1.78	–0.03(7)	0.79	–0.82	18.5	–	–	4.3	OH
NGC 4590	–7.35	–2.27	0.35(1)	0.94	0.17	10.1	76	–80	6.0	IH
NGC 4833	–8.16	–1.89	–	1.01	0.97	8.7	–221	198	5.0	IH
NGC 5024	–8.70	–2.06	–	1.04	0.81	18.3	–	–18	17.5	OH
NGC 5053	–6.72	–2.30	–	1.01	0.52	16.9	–	–	16.1	OH
NGC 5139	–10.29	–1.64	–	–	–	6.4	–271	285	1.4	IH
NGC 5272	–8.93	–1.50	0.34(8)	0.88	0.08	12.2	–56	115	10.2	IH
NGC 5286	–8.61	–1.70	–	1.02	0.80	8.4	–60	–	2.0	D/B
AM 4	–1.60	–2.07	–	–	–	25.5	–	–	16.5	OH
NGC 5466	–6.96	–2.31	0.33(9)	1.07	0.58	16.2	–	280	15.2	OH
NGC 5634	–7.69	–1.93	–	–	–	21.2	–	–	19.1	OH
NGC 5694	–7.81	–2.02	0.16(10)	1.05	1.00	29.1	–	–	17.5	OH
IC 4499	–7.33	–1.62	–	–	0.11	15.7	–	–	–6.6	OH
NGC 5824	–8.84	–1.94	–	1.00	0.79	25.8	–	–	12.0	OH
Pal 5	–5.17	–1.41	0.17(11)	–	–0.40	18.6	–	178	16.7	OH
NGC 5897	–7.21	–1.90	–	1.03	0.86	7.3	–184	149	6.2	IH
NGC 5904	–8.81	–1.33	0.38(1)	0.85	0.31	6.2	26	105	5.4	IH
NGC 5927	–7.80	–0.29	–	0.91	–1.00	4.5	8	–7	0.6	D/B
NGC 5946	–7.20	–1.29	–	0.93	–	5.8	–186	–	0.8	IH
BH 176	–4.35	–	–	0.55	–1.00	9.7	–3	–	1.2	Open Cluster
NGC 5986	–8.44	–1.63	–	0.97	0.97	4.8	–188	207	2.4	IH
Lynga 7	–6.37	–0.68	–	–	–1.00	4.2	–115	–	–0.3	D/B
Pal 14	–4.73	–1.63	–	–	–1.00	69.0	–	–	49.6	OH
NGC 6093	–8.23	–1.75	0.24(12)	1.01	0.93	3.8	–147	247	3.3	IH
NGC 6121	–7.20	–1.98	0.51(1)	0.97	–0.06	5.9	–87	196	0.6	IH
NGC 6101	–6.91	–1.18	–	1.01	0.84	11.1	–319	–	–4.2	IH
NGC 6144	–6.75	–1.82	–	1.08	1.00	2.6	–376	356	2.3	D/B
NGC 6139	–8.36	–1.71	–	0.89	0.91	3.6	–120	–	1.2	IH
Terzan 3	–4.61	–0.755	–	–	–	2.4	–23	–	1.2	D/B
NGC 6171	–7.13	–1.03	0.49(1)	0.99	–0.73	3.3	–44	69	2.5	D/B
1636–283	–3.97	–1.525	–	–	–	2.0	–	–	1.6	D/B
NGC 6205	–8.70	–1.58	0.31(8)	1.02	0.97	8.7	–199	274	5.0	IH
NGC 6229	–8.05	–1.33	–	–	0.24	29.7	–	–	2.7	OH
NGC 6218	–7.32	–1.43	0.41(1)	0.99	0.97	4.5	78	90	2.2	D/B
NGC 6235	–6.44	–1.38	–	–	0.89	4.1	–105	–	2.7	IH
NGC 6254	–7.48	–1.57	0.37(1)	0.92	0.98	4.6	–36	71	1.7	D/B
NGC 6256	–6.52	–0.62	–	–	–	1.8	–79	–	0.5	D/B
Pal 15	–5.49	–2.10	–	–	1.00	37.9	–	–	18.3	OH
NGC 6266	–9.19	–1.18	–	0.89	0.32	1.7	–31	–	0.9	D/B
NGC 6273	–9.18	–1.76	–	0.99	0.96	1.6	–351	–	1.4	D/B
NGC 6284	–7.97	–1.31	–	0.91	0.88	7.6	–39	–	2.6	D/B
NGC 6287	–7.36	–2.12	0.38(13)	1.07	0.98	2.1	271	–	1.8	D/B
NGC 6293	–7.77	–2.01	0.42(13)	–	0.90	1.4	–49	–	1.2	D/B
NGC 6304	–7.32	–0.37	–	–	–1.00	2.2	63	–	0.6	D/B
NGC 6316	–8.35	–0.36	–	–	–1.00	3.2	–105	–	1.1	D/B
NGC 6341	–8.20	–2.35	0.46(14)	1.11	0.91	9.6	79	187	4.7	IH
NGC 6325	–6.95	–1.37	–	–	–	1.1	–5	–	1.1	D/B
NGC 6333	–7.94	–1.79	–	–	0.87	1.7	–99	–	1.5	D/B
NGC 6342	–6.44	–0.49	0.38(15)	0.92	–1.00	1.7	74	–	1.5	D/B
NGC 6356	–8.52	–0.35	–	–	–1.00	7.6	–33	–	2.7	D/B
NGC 6355	–8.08	–1.33	–	–	–	1.8	147	–	0.9	D/B
NGC 6352	–6.48	–0.62	0.20(16)	0.87	–1.00	3.3	21	–	0.7	D/B
IC 1257	–6.15	–1.725	–	–	1.00	17.9	–	–	6.5	OH

Table A.1. continued.

Name	M_V	[Fe/H]	[α/Fe]	$\langle$Age$\rangle$	HBR	R_{GC} (kpc)	dV (km s^{-1})	$\Theta^\star$	Z (kpc)	Pop.
Terzan 2	–5.27	–0.29	–	–	–1.00	0.9	–308	–	0.3	D/B
NGC 6366	–5.77	–0.59	–	0.91	–0.97	5.0	144	–	1.0	IH
Terzan 4	–6.09	–1.62	0.50(17)	–	1.00	1.3	–89	–	0.2	D/B
HP 1	–6.44	–1.57	0.34(18)	–	0.75	6.1	–67	–	0.5	D/B
NGC 6362	–6.94	–1.07	–	0.94	–0.58	5.1	–81	–	–2.3	D/B
Liller 1	–	0.40	–	–	–7.63	1.8	–165	–	0.0	D/B
NGC 6380	–7.46	–0.40	–	–	–	3.2	–83	–	–0.6	D/B
Terzan 1	–4.90	–1.29	–	–	–	2.5	–139	–	0.1	D/B
Ton 2	–6.14	–0.525	–	–	–	1.4	0	–	–0.5	D/B
NGC 6388	–9.42	–0.45	0.22(1)	0.87	–0.65	3.2	–204	–	–1.2	D/B
NGC 6402	–9.12	–1.39	–	–	0.65	4.1	175	–	2.4	IH
NGC 6401	–7.90	–1.01	–	–	–	2.7	90	–	0.7	D/B
NGC 6397	–6.63	–1.99	0.36(1)	0.99	0.98	6.0	–46	87	–0.5	D/B
Pal 6	–6.81	–1.06	0.40(19)	–	–1.00	2.2	–177	–	0.2	D/B
NGC 6426	–6.69	–2.36	–	–	0.58	14.6	103	–	5.8	IH
Djorg 1	–6.26	–2.025	–	–	–	4.1	335	–	–0.5	IH
Terzan 5	–7.87	0.16	0.32(17)	–	–1.00	2.4	138	–	0.3	D/B
NGC 6440	–8.75	–0.20	–	–	–1.00	1.3	256	–	0.6	D/B
NGC 6441	–9.64	–0.44	0.21(1)	0.83	–0.76	3.9	–64	–	–1.0	D/B
Terzan 6	–7.67	–0.40	–	–	–1.00	1.6	–168	–	–0.4	D/B
NGC 6453	–6.88	–1.48	–	–	–	1.8	–13	–	–0.6	D/B
UKS–1	–6.88	–0.40	0.33(15)	–	–1.00	0.8	–	–	0.1	D/B
NGC 6496	–7.23	–0.46	–	0.87	–1.00	4.3	43	–	–2.0	D/B
Terzan 9	–3.85	–2.07	–	–	–	1.6	–29	–	–0.2	D/B
Djorg 2	–6.98	–0.525	–	–	–1.00	1.4	–	–	–0.3	D/B
NGC 6517	–8.28	–1.24	–	–	–	4.3	110	–	1.3	D/B
Terzan 10	–6.31	–0.725	–	–	–1.00	2.4	–	–	–0.2	D/B
NGC 6522	–7.67	–1.45	–	–	0.71	0.6	38	–	–0.5	D/B
NGC 6535	–4.75	–1.79	–	0.86	1.00	3.9	310	–	1.2	IH
NGC 6528	–6.56	0.07	0.24(20)	–	–1.00	0.6	–146	–	–0.6	D/B
NGC 6539	–8.30	–0.53	0.43(15)	–	–1.00	3.1	170	–	1.0	D/B
NGC 6540	–5.38	–1.225	–	–	–	4.4	16	–	–0.2	D/B
NGC 6544	–6.66	–1.47	–	0.86	1.00	5.3	27	–	–0.1	D/B
NGC 6541	–8.37	–1.82	0.43(13)	1.05	1.00	2.2	28	–	–1.4	D/B
NGC 6553	–7.77	–0.16	0.26(21)	–	–1.00	2.2	36	–	–0.3	D/B
NGC 6558	–6.46	–1.37	0.37(22)	–	0.70	1.0	187	–	–0.8	D/B
IC 1276	–6.67	–0.65	–	–	–	3.7	–80	–	0.5	D/B
Terzan 12	–4.14	–0.525	–	–	–	3.4	–67	–	–0.2	D/B
NGC 6569	–8.30	–0.72	–	–	–	2.9	25	–	–1.2	D/B
NGC 6584	–7.68	–1.50	–	0.89	–0.15	7.0	–255	181	–3.8	IH
NGC 6624	–7.49	–0.42	–	0.88	–1.00	1.2	44	–	–1.1	D/B
NGC 6626	–8.18	–1.46	–	–	0.90	2.7	27	52	–0.5	D/B
NGC 6638	–7.13	–0.99	–	–	–0.30	2.3	103	–	–1.2	D/B
NGC 6637	–7.64	–0.59	0.31(23)	0.91	–1.00	1.9	72	–	–1.6	D/B
NGC 6642	–6.77	–1.19	–	–	–	1.7	227	–	–0.9	D/B
NGC 6652	–6.68	–0.76	–	0.91	–1.00	2.8	135	–	–2.0	D/B
NGC 6656	–8.50	–1.70	0.38(24)	1.06	0.91	4.9	156	42	–0.4	D/B
Pal 8	–5.52	–0.37	–	–	–1.00	5.6	67	–	–1.5	D/B
NGC 6681	–7.11	–1.62	–	0.97	0.96	2.1	–44	–	–1.9	D/B
NGC 6712	–7.50	–1.02	–	–	–0.62	3.5	214	183	–0.5	IH
NGC 6715	–10.01	–1.44	0.16(25)	0.87	0.75	19.2	–	–	–6.5	dSph
NGC 6717	–5.66	–1.26	–	1.00	0.98	2.4	100	–	–1.3	D/B
NGC 6723	–7.84	–1.10	0.50(26)	1.01	–0.08	2.6	83	–	–2.6	D/B
NGC 6749	–6.70	–1.62	–	–	1.00	5.0	130	–	–0.3	IH
NGC 6752	–7.73	–1.55	0.43(1)	1.02	1.00	5.2	–24	21	–1.7	D/B
NGC 6760	–7.86	–0.40	–	–	–1.00	4.8	100	–	–0.5	D/B
NGC 6779	–7.38	–2.00	–	1.10	0.98	9.7	91	259	1.5	IH
Terzan 7	–5.05	–0.12	–0.03(27)	0.53	–1.00	16.0	–	–	–8.0	dSph
Pal 10	–5.79	–0.125	–	–	–1.00	6.4	58	–	0.3	D/B
Arp 2	–5.29	–1.74	0.34(28)	0.89	0.86	21.4	–	–	–10.2	dSph
NGC 6809	–7.55	–1.93	0.42(1)	1.02	0.87	3.9	–129	165	–2.1	D/B
Terzan 8	–5.05	–2.025	0.45(28)	0.97	1.00	19.1	–	–	–10.8	dSph
Pal 11	–6.86	–0.45	–	–	–	7.9	77	–	–3.5	IH
NGC 6838	–5.60	–0.82	0.40(1)	0.94	–1.00	6.7	40	40	–0.3	D/B
NGC 6864	–8.55	–1.29	–	–	–0.07	14.6	144	–	–9.0	IH
NGC 6934	–7.46	–1.56	–	0.88	0.25	12.8	328	279	–5.1	IH
NGC 6981	–7.04	–1.48	–	0.87	0.14	12.9	277	–	–9.2	IH
NGC 7006	–7.68	–1.46	0.28(29)	–	–0.28	38.8	–	–	–13.8	OH

Table A.1. continued.

Name	M_V	[Fe/H]	[α/Fe]	⟨Age⟩	HBR	R_{GC} (kpc)	dV (km s^{-1})	$\Theta^\star$	Z (kpc)	Pop.
NGC 7078	–9.17	–2.33	0.40(1)	1.01	0.67	10.4	63	92	–4.7	IH
NGC 7089	–9.02	–1.66	0.41(30)	0.96	0.96	10.4	5	306	–6.7	IH
NGC 7099	–7.43	–2.33	0.37(1)	1.08	0.89	7.1	214	324	–5.9	IH
Pal 12	–4.48	–0.81	–0.01(7)	0.64	–1.00	15.9	–	–	–14.1	dSph
Pal 13	–3.74	–1.78	–	–	–0.20	26.7	–	–	–17.5	OH
NGC 7492	–5.77	–1.69	0.34(31)	0.93	0.81	24.9	–	–	–23.1	OH

Notes. [(1)] Carretta et al. (2009b) ; [(2)] Shetrone & Keane (2000); [(3)] Yong & Grundahl (2008); [(4)] McWilliam et al. (1992); [(5)] Shetrone et al. (2001); [(6)] Ivans (2009); [(7)] Brown, et al. (1997); [(8)] Sneden et al. (2004); [(9)] McCarthy & Nemec (1997); [(10)] Lee et al. (2006); [(11)] Smith et al. 2002; [(12)] Cavallo et al. (2004); [(13)] Lee & Carney (2002); [(14)] Sneden et al. (2000); [(15)] Origlia et al. (2005); [(16)] Feltzing et al. (2009); [(17)] Origlia & Rich (2004); [(18)] Barbuy et al. (2006, corrrected upward by 0.20 dex); [(19)] Lee et al. (2004); [(20)] Carretta et al. (2001); [(21)] Cohen et al. (1999); [(22)] Barbuy et al. (2007, corrrected upward by 0.20 dex); [(23)] Lee (2007); [(24)] Marino et al. (2009); [(25)] Brown et al. (1999); [(26)] Fulton & Carney (1996); [(27)] Sbordone et al. (2007); [(28)] Mottini et al. (2008); [(29)] Kraft et al. (1998); [(30)] Russell (1996); [(31)] Cohen & Melendez (2005).

Table A.2. Comparison of our classification with the one by Mackey & van den Bergh (2005).

	Disk/Bulge	Old Halo	Young Halo	SGR
Disk/Bulge	34	36	5	–
Inner Halo	1	23	9	–
Outer Halo	1	11	15	–
dSph	–	–	1	6

Table A.3. Globular clusters of LMC, SMC, and Fornax dSph and their properties.

Name	M_V	[Fe/H]	[α/Fe]	Age	HBR
NGC 1466	–7.26	–1.76(1)	–	1.04(5)	0.41(4,6)
NGC 1754	–7.09	–1.50(1,2)	–	0.96(2,3)	0.46(3,6)
NGC 1786	–7.70	–1.76(1,2,9)	0.43(9)	1.12(2,3)	0.39(6)
NGC 1835	–8.30	–1.72(1,2)	–	0.99(2,3)	0.52(3,6)
NGC 1841	–6.82	–2.02(1)	–	0.89(8)	0.72(4,6)
NGC 1898	–7.49	–1.32(1,2,10)	0.06(10)	0.98(2,3)	–0.02(3,6)
NGC 1916	–8.24	–2.05(1,2)	–	0.93(2,3)	0.97(6)
NGC 1928	–6.06	–1.27(6)	–	0.87(13)	0.94(6)
NGC 1939	–6.85	–2.02(2,6)	–	0.94(2,3,13)	0.94(6)
NGC 2005	–7.40	–1.74(1,2,10)	0.17(10)	1.02(2,3)	0.88(6)
NGC 2019	–7.75	–1.56(1,2,10)	0.28(10)	1.20(2,3)	0.61(3,6)
NGC 2210	–7.51	–1.76(1,12,9)	0.37(9)	1.05(12)	0.61(4,6)
NGC 2257	–7.25	–1.83(1,9)	0.34(9)	1.00(5)	0.46(4,6)
Hodge 11	–7.45	–2.09(1,10)	0.38(10)	1.14(5)	0.98(4,6)
Reticulum	–5.22	–1.64(1,6)	–	0.81(13)	–0.02(4,6)
ESO121–SC03	–4.37	–0.93(12,7)	–	0.71(14)	–1.00(6)
NGC 121	–7.82	–1.46(15)	0.24(18)	0.87(15)	–0.95(6)
Lindsay 1	–5.46	–1.14(16)	–	0.58(16)	–1.00(6)
Kron 3	–6.86	–1.08(16)	–	0.51(16)	–1.00(6)
NGC 339	–5.96	–1.12(16)	–	0.47(16)	–1.00(6)
NGC 361	–6.12	–1.45(17)	–	0.63(17)	–1.00(6)
NGC 416	–7.48	–1.00(16)	–	0.47(16)	–1.00(6)
Lindsay 38	–	–1.59(16)	–	0.51(16)	–1.00(6)
Lindsay 113	–5.29	–1.38(17)	–	0.31(17)	–
Fornax 1	–5.32	–2.50(19)	0.25(19)	1.04	–0.30(6)
Fornax 2	–7.03	–2.10(19)	0.31(19)	1.01	0.50(6)
Fornax 3	–7.66	–2.40(19)	0.15(19)	1.09	0.44(6)
Fornax 4	–6.83	–1.90(20)	–	0.83	–0.42(6)
Fornax 5	–6.82	–2.20(20)	–	1.08	0.52(6)

Notes. [(1)] Suntzeff et al. (1992); [(2)] Beasley et al. (2002); [(3)] Olsen et al. (1998); [(4)] Walker (1992b); [(5)] Johnson et al. (1999); [(6)] Mackey & Gilmore (2004a); [(7)] Geisler et al. (1997); [(8)] Saviane et al. (2002); [(9)] Mucciarelli et al. (2009); [(10)] Johnson et al. (2006); [(11)] van den Bergh (2006); [(12)] Hill et al. (2000); [(13)] Mackey & Gilmore (2004b); [(14)] Mackey et al. (2006); [(15)] Glatt et al. (2008a); [(16)] Glatt et al. (2008b); [(17)] Kayser et al. (2006); [(18)] Johnson et al. (2004); [(19)] Letarte et al. (2006); [(20)] Buonanno et al. (1999).

smaller than −0.3 in HB type were classified as old halo and young halo, respectively. The Table A.2 schematically shows the comparison and emphasises the different natures of the two classifications. As (partially) expected, the matrix is not diagonal; i.e., there is not a one-to-one correlation between old halo (young halo) and inner halo (outer halo) subgroups. More in

detail, the metallicity criterion is largely responsible for such a discrepancy: had we adopted the requirement of [Fe/H] > -0.8 dex, 35 of the 36 clusters that we classified as disk/bulge and Mackey & van den Bergh as old halo should be moved into inner halo+old halo cell, while all the 5 GCs placed in the disk+young halo box should become inner halo+young halo clusters thanks to their low metallicity. However, and most important, even taking these changes into account in the relative population of the matrix cells, the resulting correspondence is not yet one-to-one. As to the inner halo GCs, 80% constitute the old halo and the remaining 20% the young halo clusters; for the outer halo GCs, the promiscuity is even greater, resulting in 40% and 60%, respectively, for old and young haloes. This is direct evidence of the strong difference between kinematics (and/or positional) criteria and the ones based only on metallicity and HB type.

One last word on the classification. While this work was in preparation, a paper by Fraix-Burnet et al. (2009) appeared, where they use a cladistic technique to divide a sample of 54 GCs into three subsamples (called Groups 1, 2, and 3 and later identify with inner halo, outer halo, and disk, respectively) on the basis of [Fe/H], M_V, $T_{\rm eff}^{\rm max}$(HB), and age. We cross-checked the assignments for the clusters in common and found good agreement only for disk clusters, and this in a limited sense. When they classify a cluster as disk, we agree (in 17 cases out of 18), but we have many other disk clusters that they instead classify in the halo subsamples. In particular, for the 19 GCs in our FLAMES sample, the two classifications agree for seven clusters and disagree for seven others (five GCs are not present in their data set). We think that the main factor producing this difference is that they ignored the kinematics, although the information is present for their sample, while our method rests on that.

To conclude, we report in Table A.3 the analogoues of Table A.1, but for the LMC, SMC, and Fornax GC systems; as in the previous case, the number in brackets corresponds to the reference (for [α/Fe], [Fe/H], age, and HBR) whose decoding is given in the Notes. The integrated magnitudes M_V for the LMC and Fornax GCs are taken from van den Bergh & Mackey (2000), while for the SMC ones were computed from the apparent magnitudes *UBV* by van den Bergh (1981), along with the distance moduli as given in those papers providing the clusters′ age (Refs. 15–17 see Table A.3). As to age, for LMC and SMC GCs, since absolute values were available (see ref. given in Table A.3), we report them to our relative scale, adopting the previous conversion of 13.5 Gyr = 1.00. For the Fornax clusters, the ages were instead derived starting from the cluster-to-cluster relative differences (ΔAge) obtained by Buonanno et al. (1998, 1999) and assuming that 1.05 = 14.2 Gyr.